Energy management and sizing of a stand-alone hybrid renewable energy system for community electricity, fresh water, and cooking gas demands of a remote island

Mim Mashrur Ahmed [a], Barun K. Das [b,*], Pronob Das [a], Md Sanowar Hossain [a], Md Golam Kibria [a]

[a] *Department of Mechanical Engineering, Rajshahi University of Engineering and Technology, Rajshahi 6204, Bangladesh*
[b] *School of Engineering, Edith Cowan University, Joondalup 6027, WA, Australia*

ABSTRACT

Research into the off-grid hybrid energy system to provide reliable electricity to a remote community has extensively been done. However, simultaneous meeting electric, freshwater, and gas demands from the off-grid hybrid energy sources are very scarce in literature. Power- to-X (PtX) is gaining attention in recent days in the energy transition scenarios to generate green hydrogen, the primary product of the process as an energy carrier, which is deemed to replace conventional fuels to reach absolute carbon neutrality. In this study, renewable–based hybrid energy is developed to simultaneously meet the electricity, freshwater, and gas (cooking gas via methanation process) demands for a remote Island in Bangladesh. In this process, an energy management strategy has been developed to use the excess energy to generate both freshwater and the hydrogen, where hydrogen is then converted to natural gas via methanation process. The PV, wind turbine, diesel generator, battery, and fuel cell have been optimized using non-dominating sorting algorithm-II (NSGA-II) to offer reliable, cost-effective solutions of electricity, freshwater, and cooking gas for the end users. Results reported that the PV/WT/DG/Batt configuration has been found the most economic configuration with the lowest COE (0.1724 $/kWh) which is 9 % lower than PV/WT/Batt configuration which has the second lowest COE. The cost of water (COW) and cost of gas (COG) of the PV/WT/DG/Batt system are also the lowest among all the four configurations and have been found 1.185 $/m^3 and 3.978 $/m^3, respectively.

1. Introduction

Establishing affordable, reliable, and clean energy systems is predominant for a developing country nation to power its infrastructure. Nations with a greater and more reliable access to the energy sources and technologies have been historically civilized and advanced at a visibly faster pace compared to their counterparts with lesser energy access [1,2]. This, combined with limited fossil fuel reserves and their environmental impact, heightens the search for cleaner and more sustainable energy sources to generate electricity. [3–5]. The useful role of pragmatic energy systems in the economic and technological advancement has been increasingly evident and acknowledged in the global perspective [6]. Despite the global setback caused by the Covid-19 outbreak, the year 2020 marks a new high for renewable capacity installation with 280 GW, 45 % higher than the previous year [7]. Hybrid energy sources (HES) with the integration of various energy

storage media reduce the inherent seasonal dependency, improves the stability of electricity supply [8–10].

The optimization of HES meeting electrical demand is extensively investigated by researchers. Several studies reported in literature where concurrently meeting the electricity and hydrogen demand [11–14], electricity, heating, and hydrogen loads [15–17], electricity and heating demand [18,19], electricity and water loads [20,21], and the electricity, water, and heating demand [22,23]. Various optimization methods have been developed to take on such a crucial challenge. These strategies can play a crucial role in sustainably scaling the HES for supplying reliable power to remote places in a cost-effective manner while guaranteeing the smallest environmental footprint. The most commonly utilized optimization methods for system sizing are the genetic algorithm (GA) [24,25], particle swarm optimization (PSO) [26–28], and hybrid optimization [29,30]. The hybrid optimization of multiple electric renewables (HOMER) software tool has extensively been used in literature for optimizing the HES for its simplicity [31,32]. Although electricity,

Nomenclature

$Batt_s(t)$	Charge level of the storage system at time t (kWh)
$Batt_s(t-1)$	Charge level of the storage system at time t-1 (kWh)
Ca_{WD}	Daily volumetric capacity (m³/day)
$C_{cap,comp}$	Capital investment cost ($/kW)
C_{CH}	Chemical cost ($)
$C_F(t)$	Fuel cost ($/h)
C_{fuel}	Fuel cost ($)
C_{ini}	Initial capital cost ($)
$C_{Mnt\text{-}RO}$	Annual maintenance cost of ROD ($/yr)
C_{MR}	Membrane replacement cost ($)
$C_{O\&M}$	Operation and maintenance cost ($)
$C_{o\&m,comp}$	Component's operation and maintenance cost ($)
C_{rep}	Replacement cost ($)
$C_{rep.comp}$	Replacement cost of the component ($)
C_{RO}	Overall RO cost ($)
C_{ROD}	Cost of ROD system ($/m³/day)
$C_{salvage}$	Present salvage value ($)
C_{WTa}	Water tank cost ($)
CC_{RO}	Capital cost of RO ($)
CC_{WTa}	Capital cost of the freshwater tank ($)
CF	Characterization factor
D_{WC}	Water production capacity (m³)
D_{WD}	Total daily volumetric freshwater demand (m³)
DOD_{SWV}	Depth of discharge of the gas storage (%)
E	Amount of energy generated or stored by the individual elements over time T (kWh)
$E_{BES}(t)$	Electricity production from battery (kWh)
$E_{DG}(t)$	Electricity production from diesel generator (kWh)
$E_{Elec}(t)$	Electricity demand (kWh)
$E_{ES,max}$	Maximum capacity of the energy storage (kWh)
$E_{ES,min}$	Minimum capacity of the energy storage (kWh)
$E_{Excess}(t)$	Excess energy (kWh)
E_L	Total delivered electrical energy (kWh)
$E_{PV}(t)$	Electricity production from PV (kWh)
$E_{ren}(t)$	Amount of generated energy by the renewable sources (kWh)
$E_{WT}(t)$	Electricity production from wind turbine (kWh)
$ED_l(t)$	Energy demand (kWh)
F_0	Fuel curve intercept coefficient (L/kWh)
F_1	Fuel curve slope (L/kWh)
F_{fuel}	Annual fuel consumption (L/yr)
f_{JC}	Job creation potential of component (jobs/kW)
f_{PV}	Derating factor of PV module (%)
FC	Faraday's constant
G_i	Incident solar radiation (kW/m²)
$G_{i,STC}$	Solar irradiance at standard test conditions (kW/m²)
$H_{WD}(t)$	Water demand at hour t (m³)
i	Discount rate (%)
$I_{elec}(t)$	Current passing through electrolyzer at hour t (A)
JC	Job creation (jobs)
K_{SWV}	Gas storage pressure (MPa)
LF_{comp}	Project lifetime (yr)
LPS	Loss of power supply (kWh)
$M_{elec}(t)$	Hydrogen production at hour t (mol)
$\dot{m}_{fuel}(t)$	Fuel consumption rate of generator at time t (L/h)
$M_{meth}(t)$	Methane production via methanation process at hour t (mol)
$M_{meth.max}$	Maximum methane production (mol)
$M_{SWV}(t)$	Amount of methane in the storage at hour t (mol)
MC_{RO}	Operation and maintenance cost of RO ($)
N_{comp}	Number of optimal components
N_{IN}	Number of inverters

N_{Me}	Number of annual membrane replacement
$N_{rep-comp}$	Number of replacements required for a component during its lifetime
$NOCT$	Nominal operating cell temperature (°C)
P	Total capacity of the component (kW)
P_D	ROD Installed power (kW)
$P_{DEM}(t)$	Power requirement for desalination (kW)
P_{DES}	Instantaneous power utilization of the ROD unit (kW)
P_{DI}	ROD unit nominal load (kW)
$P_{elec}(t)$	Power consumed by the electrolyzer at hour t (kW)
$P_{elec,rated}$	Electrolyzer's rated power (kW)
$P_G(t)$	Amount of diesel generator production at time t (kW)
P_{G_max}	Maximum power generated by the hybrid system (kW)
$P_{in}(t)$	Input power of the inverter (kW)
P_{IN_max}	Maximum power that can be supplied by the inverter (kW)
P_{MD}	Minimum ROD load (kW)
$P_{out}(t)$	Output power of the inverter at time t (kW)
P_{PV}	Power output of PV (kW)
$P_{PV,rated}$	Rated capacity output from PV array (kW)
P_R	Nominal power of diesel generator (kW)
P_{rated}	Rated power of wind turbine (kW)
P_{WT}	Power output of the wind turbine (kW)
$Q_{C,SWV}(t)$	Methane charging volume at hour t (m³)
$Q_{D,SWV}(t)$	Methane discharging volume at hour t (m³)
$Q_{load}(t)$	Gas load demand at hour t (m³)
$Q_{SWV}(t+1)$	Methane stored in the storage at hour t + 1 (m³)
$Q_{SWV,max}$	Maximum gas storage (m³)
R	Gas constant (atm/mol.K)
S_{DC}	Average desalination specific energy consumption (kWh/m³)
$SOC_{SWV,max}$	Upper limit of the state of charge of the gas storage (%)
$SOC_{SWV,min}$	Lower limit of the state of charge of the gas storage (%)
T_{amb}	Environment temperature (°C)
T_C	PV cell temperature (°C)
$T_{C,STC}$	PV cell temperature under standard test conditions (25)°C
T_{SWV}	Gas storage temperature (°C)
TC_{Chem}	RO chemical cost ($)
TC_{MR}	RO replacement cost ($)
V	Velocity of wind turbine at any instant (m/s)
V_c	Cut-in velocity of the wind turbine (m/s)
V_f	Furling velocity of wind turbine (m/s)
V_{elec}	Working voltage (V)
V_{rated}	Rated velocity of wind turbine (m/s)
V_{WTa}	Volumetric capacity of the water tank (m³)
α_p	Power temperature coefficient (/°C)
ψ	Lifetime CO₂ emission equivalent (kg CO₂-eq/kWh)
σ	Hourly self-discharge rate of the battery (%)
$\tau\alpha$	PV module effective transmittance-absorptance
η_{bc}	Charging efficiency (%)
η_{bf}	Discharging efficiency (%)
η_{INV}	Inverter efficiency (%)
η_{meth}	Hydrogen to methane conversion efficiency
η_{PV}	PV cell efficiency (%)
η_V	Voltage efficiency (%)

Abbreviations

ANN	Artificial Neural Network
ARMA	Autoregressive Moving Average
Batt	Battery
BSO	Brain Storm Optimization
CF	Characterization Factor
CH₄	Methane
CNG	Compressed Natural Gas

CO	Carbon Monoxide	MOGA	Multi-Objective Genetic Algorithm
CO_2	Carbon di Oxide	NOCT	Nominal Operating Cell Temperature
COE	Cost of Energy	NPC	Net Present Cost
COW	Cost of Water	NSGA	Non-Dominated Sorting Genetic Algorithm
CS	Chaos Search	O_2	Oxygen
DALY	Disability Adjusted Life Years	O&M	Operation and Maintenance
DES	Damaging Effect on Ecosystem	PEM	Proton Exchange Member
DG	Diesel Generator	PSO	Particle Swarm Optimization
DHH	Damage on Human Health	PtX	Power to X
EE	Excess Energy	RF	Renewable Fraction
GA	Genetic Algorithm	RL	Reverse Osmosis Load
GHG	Greenhouse Gas	RNN	Recurrent Neural Network
GL	Gas Load	RO	Reverse Osmosis
GWO	Grey Wolf Optimization	ROD	Reverse Osmosis Desalination
H_2	Hydrogen	SAARC	South Asian Association for Regional Cooperation
HES	Hybrid Energy Sources	SNG	Solidified Natural Gas
HOMER	Hybrid Optimization of Multiple Electric Renewables	SOC	State of Charge
HRES	Hybrid Renewable Energy Sources	SWV	Single-Well-Vertical
HSA	Harmony Search Algorithm	TSA	Tabu Search Algorithm
LCE	Life Cycle Emission	UGS	Underground Inventory
LNG	Liquefied Natural Gas	WCA	Water Cycle Algorithm
LPSP	Loss of Power Supply Probability	WHO	World Health Organization
MATLAB	Matrix Laboratory	WT	Wind Turbine
MFO	Moth Flame Optimization	$Q_{SWV}(t)$	Methane stored in the storage at hour t (m^3)
MILP	Mixed-Integer Linear Programming	ZDNM	Zero-Dimensional Numerical Model

hydrogen, and heat demand can be satisfied using HOMER software tool, the methanation process is not integrated within it. Therefore, in this study, non-dominating sorting algorithm-II (NSGA-II) has been used to meet multiple demands such as electricity, freshwater, and cooking gas in a stand-alone application. Newly developed intelligent techniques including water cycle algorithm [33], firefly algorithm [34], moth-flame optimization [33,35], flower pollination algorithm [36], and crow search algorithm [37] are used for sizing the HES. Most optimization techniques considers cost minimization as a single objective function or a multi-objective function(s) including cost and environmental emissions in order to fulfill a given load reliability [38]. The loss of power supply probability (LPSP) is a commonly used reliability index in this context for sizing of while supplying electric demand only [39–42].

For stand-alone application of HES systems, the focus to date has been to deploy them for meeting power (only) requirements, without that much inclination on assessing the prospect of their use to meet thermal loads. Researchers have made substantial efforts to develop optimal HES, which can be reliable and produce clean energy with a reasonable cost. Although hybridization delivers greater reliability of power supply, the system generates a large portion of excess energy, which is usually dumped if not recovered [43–46]. Liu et al. [47] optimized a HES system (PV/DG/Batt) to meet the energy and fresh water demand in Iran. The system was optimized based on cost, reliability, and environmental impact and authors determined a cost of energy (COE) of 0.265 $/kWh and a cost of water (COW) of 1.06 $/$m^3$. Although the study examined the economic and environmental indicators under a reliability constraint, social factors such as job creation and human development index have not been reported. Moreover, excess energy generation from the HES has not investigated, which would be potential sources for further use for meeting heating and gas generation. A case study in Egypt optimized the HES system meet electricity demand along with water and heating demand [22] and found the best configuration had the COE of 0.089 $/kWh with a 36.50 % CO_2 reduction. The study used HOMER software tool to meet the heating, electricity, and water demand; however, optimizing a HES under a certain reliability is not straightforward in this software. In addition to that the water demand cannot be met by the excess energy generated from HES using HOMER software tool. In the a grid integrated HES, additional energy after

meeting the demand either can be used to charge the battery/stored in the H_2-based storage or sell to the grid [48,49]. Nevertheless, in a grid independent HES, the excess energy after meeting the load demand and storing energy, the surplus is then dumped [50]. In a HES system, the excess energy can be used for different applications such as meeting the thermal demand, due to the limitations associated with supplying more electricity [23]. In another study, authors performed simulation to supply electricity to the households of Zimbabwe consisting PV, DG and water turbines [51] and reported that the optimized system generates around 16,500 kWh/year extra energy, which may meet the electricity requirement of approximately 11 families in a year. Therefore, in any HES system a large amount of excess energy is produced which will be wasted if not utilized in other applications. A common misconception is that this excess energy increases the reliability of the system without affecting the overall cost of the system [52]. As excess energy is produced while energy demand is low, it will not boost system reliability until a bigger capacity storage device is installed. Ampah et al. [53] developed HESs of PV/WT/DG/BES using HOMER to meet the electric and hydrogen demand for coal mine sites in China with a LCOE of 0.136 $/kWh and the hydrogen cost of 12.14 $/kg. However, the HES generated around 27 % of excess energy, which is dumped. In a grid integrated HES can easily sell the excess energy to the grid, but in the grid independent system either one can utilize to produce heating, cooling, water or dumped. However, this requires developing an energy management strategy (EMS) to use the excess energy for the generation of freshwater and natural gas via methanation. Recent studies on HES system meeting multiple load demands are summarized in Table 1. It is clearly evident from Table 1 that most of the studies investigated the HES system meeting multiple load demands use HOMER software tool. However, in the HOMER software, one can only optimize HESs to meet the heating, water, electricity, and hydrogen demand. In this context, when a renewable hybrid system meeting demands of electricity demand, freshwater, and natural gas demands, an EMS needs to develop so as to use the excess energy.

Power to X (PtX) has been first introduced in 2008 and from then it has become the topic of interest of the researchers due to its reliability while handling excess power and converting to useful forms of energy [54]. Moreover, PtX allows integration of multiple renewable energy

Table 1

Recent works on the HES sizing meeting multiple load demands.

HES configurations	Study area	Methods	Supply loads	Design criteria	Best outcomes	Study year	Ref.
PV/WT/FC/BES	Iran	TRNSYS	Electricity, Hydrogen, Water	Life cycle cost	LCC: 674278.4$	2023	[64]
PV/DG/FC/BES/Grid	Saudi Arabia	HOMER	Electricity, Hydrogen, Water, Heat	Economy, environmental impact	COE: 0.008 $/kWh, CO_2: 5364 kg/yr, IRR: 2.57 yr	2023	[65]
PV/WT/FC	Egypt	HOMER	Electricity, Hydrogen	Cost	LCOE: 0.308 $/kWh, COH: 3.73 $/kg	2023	[66]
PV/WT/BES	Pakistan	HOMER	Electricity, Hydrogen	Cost	LCOE: 0.465 $/kWh, IRR: 17.3 %, Payback period: 2.3 yr	2023	[67]
PV/WT/FC/BES	Japan	MILP	Electricity, Hydrogen	Economy, environmental impact	CO_2: 56.1 ton, Cost: 4.3 Million yen	2023	[68]
WT/FC/Solar thermal	Iran	GA	Electricity, Hydrogen, Water	Cost	Cost rate: 48.6$/h ($H_2$)Coat rate: 48.3$/h (water)	2023	[69]
PV/DG/BES	Iran	TSA, HSA	Electricity, Water	Economy, environmental impact, reliability	TNAC: 13,900.5 $ LCOE: 0.2650 $/kWh COW: 1.0599 $/m^3 CO_2: 20,503.6 kg/yr	2022	[47]
PV/WT/CHP-MTG/DG/ TLC/BES/BLR	Egypt	HOMER	Electricity, Heat, Water	Economy, environmental impact	NPC: 1.54 M$ LCOE: 0.089 $/kWh CO_2: 36.5 % reduction	2021	[22]
PV/BG/PHES/BES	India	WCA, MFO	Electricity, Water	Cost	NPC: 0.813 M$ LCOE: 0.4864 $/kWh	2019	[33]
PV/WT/PHES/BES	China	PSO	Electricity, Water	Sensitivity, cost	LCOE: 0.196 $/kWh	2021	[70]
PV/WT/BES/CHP	Iran	PSO, ANN	Electricity	Economy, environmental impact	CO_2 emission: 35620 kg/yr Total Cost: 2367 $/yr	2021	[23]
PV/WT/BES/Solar thermal collectors	Denmark Spain	MOGA	Electricity, Water	Economy, environmental impact	N/A	2020	[71]
PV/WT/DG/BES	Turkey	HOMER	Electricity, Water	Economy, environmental impact	LCOE: 0.308 $/kWh NPC: 152,672 $ CO_2 emission: 3925.87 kg/yr COW: 2.20 $/m^3	2018	[72]
PV/WT/DG/BES	Spain	HOMER	Electricity, Water	Economy, environmental impact	LCOE: 0.404 $/kWh CO_2 emission: 82,651 kg/yr reduction	2019	[73]
PV/WT/BES/Grid	UK	RNN, EMP	Electricity, Water	Reliability, cost, environmental impact	TNAC: 21,808 $	2019	[74]
PV/WT/DG/BES	Egypt	HOMER	Electricity, Water	Economy, environmental impact	LCOE: 0.107 $/kWh NPC: 502,662 $ CO_2 emission: 94 % reduction	2019	[21]
Solar thermal collector/ geothermal	Iran	MOGA	Electricity, Water, Hydrogen	Cost, exergy	Cost rate: 63.89 $/h Exergy efficiency: 21.63 %	2020	[75]
PV/WT/BES	Egypt	PSO-GWO	Electricity, Water	Economy, environmental impact	COW: 1.08 $/m^3 CO_2 emissions: 2227 kg/yr	2018	[76]
PV/WT	Spain	BSO	Electricity, Water	Cost	LCOE: 7.34 €/MWh	2020	[77]
PV/DG/BES/RO	Iran	TSA	Electricity, Water	Economy, environmental impact	LCC: 28,130 $ LCOE: 0.3975 $/kWh COW: 1.59 $/m^3 CO_2 emission: 31,380 kg/y	2018	[78]
PV/WT/BES/DG	N/A	HOMER	Electricity, Water	Cost	LCOE: 0.144 $/kWh RF: 88 % NPC: 69.05 M$/	2020	[79]
PV/WT/DG/BES	Egypt	HOMER	Electricity, Water	Economy, environmental impact	LCOE: 0.2252 $/kWh CO_2 emission: 15,658 kg/yr COW: 1.10 $/m^3	2020	[80]

systems and allow the reduction of fossil fuel usage [55]. PtX is the general term and can refer to different pathways like, power to gas, power to liquid or gaseous fuels, power to heat and power to chemicals [56]. The most common PtX pathways include power to hydrogen, power to power, power to natural gas and power to ammonia [57]. In power to hydrogen pathway, hydrogen is produced by the electrolysis of water. This pathway has several benefits as it implies no carbon emission and the process has low irreversibility [57]. The primary obstacle to the widespread use of this technology is the higher cost of electrolyzer and its lower capacity. It is expected to reduce the electrolyzer and its balance of plant prices by 230–380 $/kW by 2030 [58]. The reduction of components price and the ongoing technological advancement would allow the green hydrogen production cost at a competitive price with the existing fossil fuel price. Methantor may be used in PtX technology to produce synthetic natural gas (SNG). Methanation can fulfill both the gas and heat demand if implemented [59]. Flexible PtX significantly improves the HES energy efficiency by minimizing the curtailment and battery charging losses and has the potential to reduce the HES sizing and costs [60]. Li et al. [61] performed the performance analysis of power to SNG pathway in a HES system using a time-domain simulation. In another work, Xu et al. [62] optimized a PV/Batt/Eletrolyzer/Methanator system to ensure maximum reliability. Through optimization the authors could use both power and gas simultaneously to handle the excess energy generated during the process. However, the system did not include a meeting a freshwater demand and the social indicators have also not been studied in their investigation. Cost optimization using MILP algorithm was performed for a HRES system incorporating power to SNG technology in a study done by [63]. The authors found that the

cost associated with battery is larger than the alkaline electrolyzer. Although few research have been conducted in recent years emphasizing the benefits of PtX technologies, there is no analysis as per the author's knowledge that illustrates the benefits of PtX under the sustainable development goals.

This study, for the first time, considers covering three types of demand typically incurred in a community: electricity, water, and cooking gas, utilizing solely renewable clean energy sources. Considering the above-mentioned literature review, a hybrid system consisting of PV module, wind turbine, battery, and backup generators has been modeled to meet electrical demand as well as water and cooking demands through utilizing the excess energy.

2. Materials and methods

A schematic diagram of the proposed HES is shown in Fig. 1. The system is made up of PV and wind turbines as primary energy sources, a battery bank for energy storage, a diesel generator for backup power, a reverse osmosis desalination (ROD) unit, a methanation unit with an electrolyzer and gas storage, and an inverter.

2.1. Study area

The research focuses on Saint Martin, only coral island in Bangladesh, which is located in Teknaf, Cox's bazar district (longitude 20°37′58″N and longitude 92°19′12″E). The island is 3.6 m above sea level. Fishing is the only source of income and life here, and 12 % of the population is illiterate. The area has no line gas supply and grid electricity supply, so diesel generator is the only energy source. Drinking water scarcity is one of the major problems in the area due to high salty water.

2.2. Load assessment

The load of the community is the primary input electric load of the selected region as presented in Table 2. Here, in this work, 100 households, 8 restaurants, 10 hotels, 30 shops, 5 small business centers, one primary school and one health center are considered for community load based on expert opinions, personal communications, and domestic patterns in summer and winter. The similar approached has been reported in Ref [81,82] to determine the remote area electric load demand. The daily loads of the community are 1130 kWh/day (summer) and 835.34 kWh/day (winter). Maximum load demand comes from households which are 602 kWh/day (summer) and 469 kWh/day (winter). process as reported in Fig. 2.

According to the United Nations and the World Health Organization (WHO), one individual requires freshwater of 20 L everyday [20]. In the current study, 1000 people require 20 m^3 of fresh water to meet their freshwater needs. Furthermore, in a ROD system, 1 m^3 of freshwater requires 4.38 kWh of electricity [20]. As a result, desalinating 20 m^3 of water requires 87.6 kWh/day of energy. Furthermore, the average demand for biogas each meal per person is projected to be 0.11 m^3 [83]. Therefore, assuming three meals per day, a total 330 m^3/day biogas is required for cooking purposes for the study area.
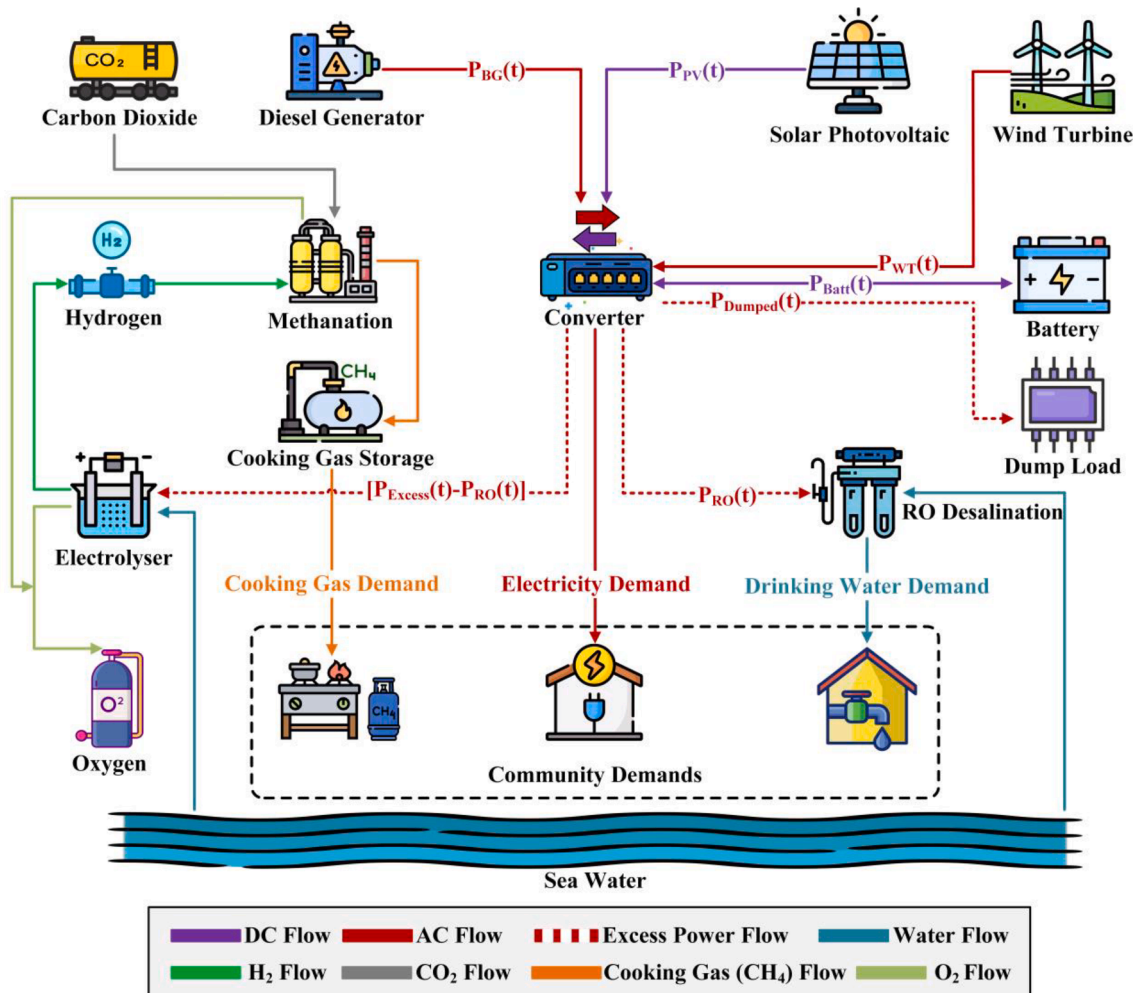

Fig. 1. Schematic layout of the proposed HES.

Table 2
Estimation of the daily load demand for the community.

| Load	Rating (W)	No. of use	March-October (Summer)		November-February (Winter)	
			Operating hour (h/day)	kWh/day	Operating hour (h/day)	kWh/day
(A) House						
Mobile Charger	6	3	4	0.072	4	0.072
Fan	70	2	10	1.400	–	–
Refrigerator	150	1	24	3.600	24	3.600
TV	100	1	5	0.500	5	0.500
CFL bulb	25	3	6	0.450	7	0.525
Total load single house				6.02		4.69
Total load for 100 houses				**602**		**469**
(B) Restaurant						
Mobile Charger	6	2	4	0.048	4	0.048
Fan	70	6	6	2.520	–	–
Refrigerator	150	1	24	3.600	24	3.600
TV	100	1	5	0.500	5	0.500
CFL bulb	25	10	6	1.500	6	1.500
Total load for single restaurant				8.170		5.650
Total load for 8 restaurants				**65.360**		**45.200**
(C) Hotel						
Mobile Charger	6	20	4	0.480	4	0.480
Fan	70	20	8	11.200	–	–
Refrigerator	150	2	24	7.200	24	7.200
TV	100	15	4	6.000	4	6.000
CFL bulb	25	40	6	6.000	7	7.000
Water Pump	1500	1	2	3.000	2	3.000
Total load for a single hotel				33.880		23.680
Total load for 10 hotels				**338.800**		**236.800**
(D) Shops (30) + Small Business Centers (5) + Primary School (1) + Health Center (1)						
Mobile Charger	6	40	4	0.960	4	0.960
Fan	70	60	10	42.000	–	–
Refrigerator	150	10	24	36.000	24	36.000
TV	100	10	5	5.000	5	5.000
CFL bulb	25	100	7	17.500	8	20.000
Water Pump	746	6	5	22.380	5	22.380
Total Summation of (D)				**123.840**		**84.340**
Grand Total (A + B + C + D)				**1130.000**		**835.340**

2.3. Renewable energy resource data

Because of its geological location, the study area has more daylight hours and a higher wind velocity than other areas in Bangladesh. The solar irradiance data as well as the wind speed data are for the study area are received from the NASA within the HOMER software. The mean wind speed and solar irradiation are 4.85 m/s and 4.80 kWh/m^2/day, respectively. The hourly temporal resolution of wind speed and solar irradiation is used in this optimization.

2.4. Modelling of HES

The HES includes a methanation unit, PV module, diesel generator, wind turbine, battery bank, and RO unit. The technical specifications and the related costs of the components are summarized in Table 3. For each component, the following subsections provide mathematical modeling, technical, and economic data:

2.4.1. Electrolyzer

Electrolyzer converts water into hydrogen and oxygen which contains an anode, a cathode, and a tank body. Proton exchange member (PEM) divides the cathode and anode chamber. The electrolyzer splits water into hydrogen and oxygen using electrical energy. The chemical process of the system is follows [85]:

$$H_2O + Electricity \rightarrow H_2 + \frac{1}{2}O_2$$
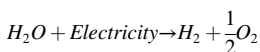
The maximum hydrogen generation is determined by the electrolyzer's rated power, which is an optimization variable in the study. Total hydrogen production by the electrolyzer can be calculated from the Equations (1) – (4) [62].

$$M_{elec}(t) = \left[\frac{I_{elec}(t)}{2 \times FC}\right] \times 3600 \tag{1}$$

$$P_{elec}(t) = I_{elec}(t) \times V_{elec} \tag{2}$$

$$V_{elec} = \left[\frac{V_H}{\eta_V}\right] \times 100\% \tag{3}$$

$$0 \leq P_{elec}(t) \leq P_{elec,rated} \tag{4}$$

where, $M_{elec}(t)$ refers to hydrogen production at hour t, FC is the Faraday's constant, $I_{elec}(t)$ is the current passing through electrolyzer at hour t, $P_{elec}(t)$ is the power consumed by the elctrolyzer at hour t, $P_{elec,rated}$ is the electrolyzer's rated power, V_{elec} is the working voltage and η_V is the voltage efficiency. Additionally, V_H refers to the hydrogen decomposition voltage (1.48 V) [86].

2.4.2. Methanation

Methanation refers to the production of methane by taking carbon dioxide from the atmosphere and hydrogen from the electrolyzer. The chemical process of methanation is described here, and it is based on the Sabatier reaction [87].

$$CO_2 + 2H_2 \rightarrow CH_4 + O_2$$
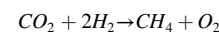
The rated power of the PEM electrolyzer and the methanation are considered to be the same for producing maximum hydrogen. The hydrogen produced in the electrolyzer is fed here to produce methane. The amount of methane produced is associated with the size of the electrolyzer. Equations (5 and 6) represent the methane production at hour t and the limits of the methanation, respectively [62].
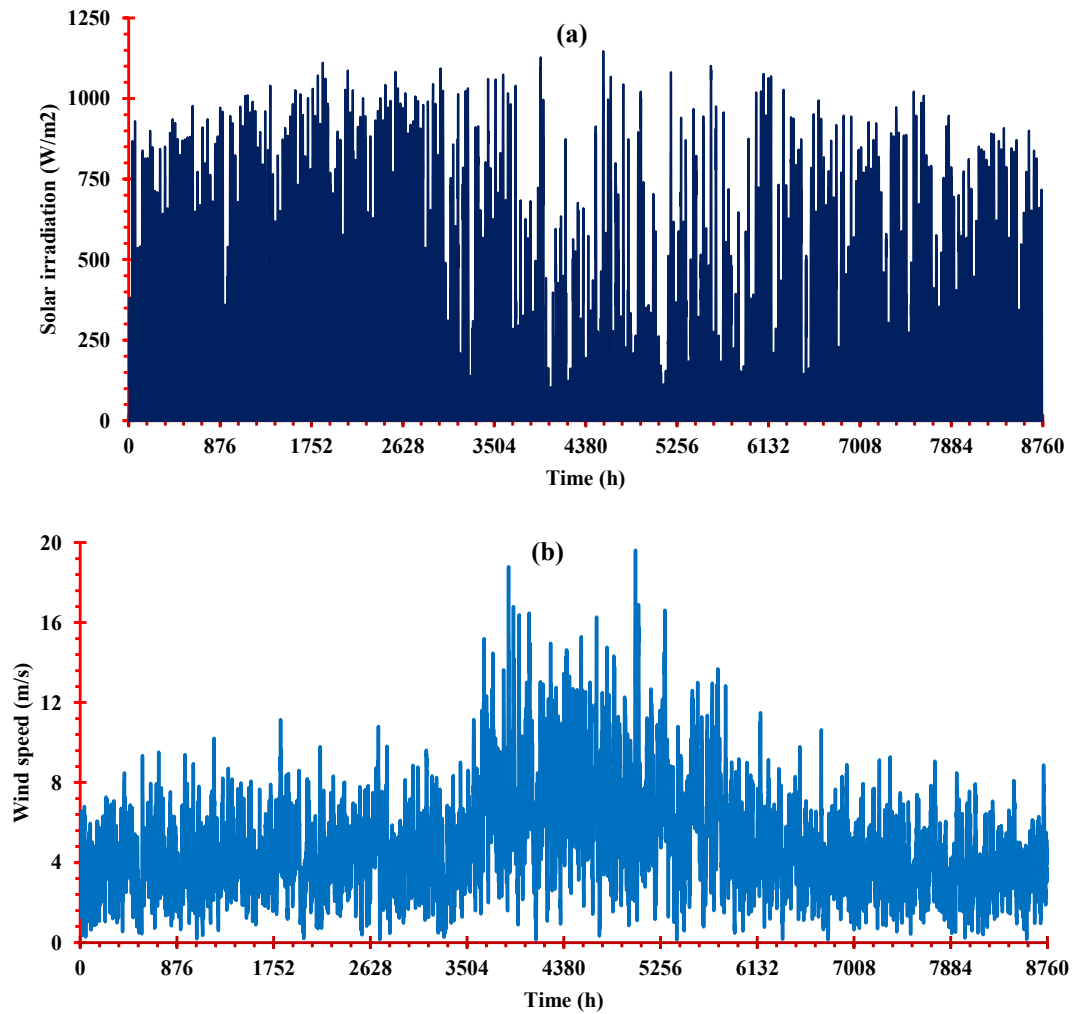
Fig. 2. Time resolved (hourly) (a) solar irradiation and (b) wind velocity for Saint Martin, Bangladesh.

$$M_{meth}(t) = \eta_{meth} \times M_{elec}(t) \qquad (5)$$

$$0 \leq M_{meth}(t) \times \frac{\eta_{meth} \times \eta_V \times P_{elec,rated}}{2 \times 1,48 \times 100\%} \times 3600 = M_{meth,max} \qquad (6)$$

where, $M_{meth}(t)$ represents methane production via methanation process at hour t, η_{meth} is the hydrogen to methane conversion efficiency and $M_{meth,max}$ is the maximum methane production.

2.4.3. Gas storage

Several ways can be followed to store the generated methane, such as compressed natural gas (CNG), underground inventory (UGS), solidified natural gas (SNG), liquefied natural gas (LNG) and absorbed natural gas [88]. In the present study, a single-well-vertical (SWV) gas storage is used from the literature of the previous study [89] with the aid of methane gas storage. In this work, methane loss from the storage is neglected for simplification. Equation (7) is used to convert molecular mass of methane (16 g/mol) to the liter of gas storage [62].

$$Q_{C,SWV}(t) = \frac{M_{SWV}(t) \times T_{SWV} \times R}{1000 \times K_{SWV}} \qquad (7)$$

where, K_{SWV} represents the gas storage pressure, $M_{SWV}(t)$ represents the amount of in the storage at hour t. Besides, $Q_{C,SWV}(t)$ refers to the methane charging volume at hour t, T_{SWV} is the gas storage temperature and R is the gas constant. The amount of gas stored in the storage depends on time and thus, a state variable is used to denote the volume of methane contained in the storage and can be represented as:

$$Q_{SWV}(t+1) = \begin{cases} Q_{SWV}(t) + Q_{C,SWV}(t) \\ Q_{SWV}(t) - Q_{D,SWV}(t) \end{cases} \qquad (8)$$

Here, $Q_{SWV}(t)$ represents the methane stored in the storage at hour t and $Q_{D,SWV}(t)$ is the methane discharge form the storage at hour t. The lower and upper limits of the stored gas can be determined from the Equation (9) and the minimum state of charge of the gas storage is found from Equation (10) [62]. The availability of gas stored in the storage determines the gas output of the gas storage.

$$Q_{SWV,min} \leq Q_{SWV}(t) \leq Q_{SWV,max} \qquad (9)$$

$$SOC_{SWV,min} = 1 - DOD_{SWV} \qquad (10)$$

where, $Q_{SWV,max}$ and $Q_{SWV,min}$ represent the maximum and minimum gas storage, respectively. Additionally, $SOC_{SWV,min}$ is the state of charge of the gas storage and the storage depth of discharge is represented by DOD_{SWV}. Charging and discharging are distinguished by using positive and negative sign, respectively. The methane flow (charging/discharging) is limited by:

$$Q_{load}(t) \leq Q_{D,SWV}(t) \leq 0 \qquad (11)$$

$$0 \leq Q_{C,SWV}(t) = \frac{M_{meth,max} \times T_{SWV} \times R}{1000 \times K_{SWV}} \qquad (12)$$

Here, $Q_{load}(t)$ represents the gas load demand at hour t.

Table 3

Technical specifications and related costs of the HES.

Component	Particulars	Specifications	Ref.
PV Module (327 W)	Efficiency	20.40 %	[20]
	Operating Voltage	54.70 V	
	Operating Current	5.98 A	
	Derating Factor	90 %	
	Temperature Coefficient	0.43/°C	
	Initial Cost	1300 $/kW	[18]
	O&M Cost	20 $/year	
	Life	25 years	
Wind Turbine (10 kW)	Cut-in Velocity	2.75 m/s	[84]
	Rated Velocity	6.5 m/s	
	Cut-off Velocity	20 m/s	
	Hub Height	20 m	
	Life	20 years	
	Capital Cost	2300 $/kW	
	O&M Cost	20 $/year	
	Replacement Cost	1500 $/kW	
Lead-Acid Battery (6.94 kWh, 1156 Ah)	Initial Cost	1100 $/unit	[84]
	Replacement Cost	10 $/unit-yr	
	O&M Cost	1000 $/unit-yr	
	Life	12 years	
	Charging Rate	80 %	[78]
	Discharging Rate	100 %	
	Self-discharge Rate	0.02 %	
Diesel Generator (30 kW)	Capital Cost	220 $/kWh	[20]
	O&M Cost	0.03 $/h	
	Replacement Cost	200 $/kW	
	Life	15,000 h	
Reverse Osmosis System	O&M Cost	0.2 $/m³	[78]
	Water Storage Tank	255.4 $/m³	
	Chemical Cost	0.06 $/m³	
	Capital Cost	532 $/m³/day	
	Replacement Cost	0.06 $/m³	
Inverter (1 kW)	Capital Cost	300 $/kW	[20]
	O&M Cost	10 $/year	
	Replacement Cost	300 $/kW	
	Efficiency	95 %	
	Life	15 years	
Electrolyzer (1 kW)	Capital Cost	500 $/kW	[62]
	O&M Cost	10 $/year	
	Replacement Cost	300 $/kW	
	Life	10 years	
Methanation (1 kW)	Capital Cost	400 $/kW	[62]
	O&M Cost	10 $/year	
	Replacement Cost	200 $/kW	
	Life	10 years	
Gas storage (20 m³)	Capital Cost	20 $/m³	[62]
	O&M Cost	4 $/m³/year	
	Life	20 years	

2.4.4. Photovoltaic array

The power output and PV cell temperature can be estimated from the Equations (13) and (14), respectively [19].

$$P_{PV} = P_{PV,rated} \times f_{PV} \times \left(\frac{G_i}{G_{i,STC}} \right) \left[1 + \alpha_p \left(T_C - T_{C,STC} \right) \right] \tag{13}$$

$$T_C = T_{amb} + G_i \times \left[\frac{NOCT - 20}{800} \right] \left(1 - \frac{\eta_{PV}}{\tau\alpha} \right) \tag{14}$$

where, $P_{PV,rated}$ represents the rated capacity output from PV array in kW, f_{PV} refers to the derating factor which is taken as 90 %, G_i is the incident solar radiation in kW/m^2, $G_{i,STC}$ denotes the incident solar irradiance in kW/m^2 at standard test conditions, α_p refers to the power temperature coefficient $(/°C)$, T_C represents the PV cell temperature $(25°C)$, and $T_{C,STC}$ indicates the temperature of the PV cell under standard test conditions which is $(25°C)$. Additionally, T_{amb} is environment temperature $(°C)$, NOCT is the nominal operating cell temperature, $\tau\alpha$ is the PV module effective transmittance-absorptance which is 0.90 in this study, and η_{PV} is the PV cell efficiency (%).

2.4.5. Wind turbine modelling

The electrical power output of the wind turbine can be estimated from the following Equation [90].

$$P_W(t) = \begin{cases} 0 & for & V < V_c \\ a + b \times V^z & for & V_c \leq V \leq V_r \\ P_{rated} & for & V_r < V \leq V_f \\ 0 & for & V > V_f \end{cases} \tag{15}$$

where, P_{rated} is the rated power in kW, V_c is the cut-in velocity of the wind turbine (m/s), V_f represents the furling wind velocity (m/s), V_r refers to the rated velocity (m/s), and z is the Weibull shape parameter.

The coefficients a and b can be determined by using Equations (16) and (17), respectively.

$$a = \frac{P_{rated} \times V_c^z}{V_c^z - V_r^z} \tag{16}$$

$$b = \frac{P_{rated}}{V_r^z - V_c^z} \tag{17}$$

2.4.6. Battery modelling

The charge level of the storage system and charging and discharging states are determined from the Equations (18) and (19), respectively [78].

$$Batt_s(t) = Batt_s(t-1) \times (1 - \sigma) + \left[E_{ren}(t) - \frac{ED_l(t)}{\eta_{INV}} \right] \eta_{bc} \tag{18}$$

$$Batt_s(t) = Batt_s(t-1) \times (1 - \sigma) - \left[\frac{ED_l(t)}{\eta_{INV}} - E_{ren}(t) \right] \Big/ \eta_{bf} \tag{19}$$

where, $Batt_s(t)$ and $Batt_s(t-1)$ are the charge levels of the storage system at time t and $t-1$, respectively. $E_{ren}(t)$ refers to the amount of generated energy by the renewable sources, η_{INV} refers to the inverter efficiency, σ represents the hourly self-discharge rate, η_{bc} represents the charge efficiency, and η_{bf} is the discharging efficiency. Charging state limit can be determined using equation (20) [78]:

$$Batt_{s,min} \leq Batt_s(t) \leq Batt_{s,max} \tag{20}$$

where, $Batt_{s,max}$ represents the maximum charge state (nominal capacity) and $Batt_{s,min}$ refers to the minimum state of charge (20 % of the maximum state). In this study, a lead acid battery with the lifetime of 12 years is considered [91].

2.4.7. Diesel generator

The fuel price is assumed as 0.77 $/L. The fuel consumption rate (L/h) and consumption cost ($/h) of the diesel generator can be determined from the following equations [92]:

$$\dot{m}_{fuel}(t) = F_0 \times P_G(t) + F_1 \times P_R \tag{21}$$

$$C_F(t) = \dot{m}_{fuel}(t) \times P_{fuel} \tag{22}$$

where, F_0 refers to the fuel curve intercept coefficient which is 0.246 L/kWh, F_1 is the fuel curve slope (0.08145 L/kWh), P_{fuel} is the fuel price ($/L), and C_F represents the cost associated with the fuel consumption.

2.4.8. Reverse Osmosis (RO) system

The RO system is used to supply pure drinking water. The system requires 20 m³/day of water and two membrane replacements each year [78]. The total power requirement for desalination (P_{DEM}) is determined using equation (23) [78]:

$$P_{DEM}(t) = H_{WD}(t) \times S_{DC} \tag{23}$$

where, H_{WD} refers to the water demand (m^3) at hour t and S_{DC} is the average desalination specific energy consumption (kWh/m^3). The water production capacity, load constraint and the volumetric capacity of the water tank are determined from the following sets of equations [78]:

$$D_{WC} = 24\left(\frac{P_D}{S_{DC}}\right) \tag{24}$$

$$P_{MD} \leq P_{DES} \leq P_{DI} \tag{25}$$

$$V_{WTa} = 2D_{WD} \tag{26}$$

Here, D_{WC} is the water production capacity, P_D refers to the installed power, P_{DI} represents the ROD unit normal load, P_{DES} refers to the instantaneous power utilization of the ROD unit, P_{MD} is the minimum load, V_{WTa} represents the volumetric capacity of the water tank, and D_{WD} is the total daily volumetric freshwater demand. Note that, the minimum operation limit is set to 25 % of the nominal power of the ROD.

2.4.9. Inverter modelling

Output power of the inverter (P_{out}) and the number of inverters (N_{IN}) can be determined from the Equations (27) and (28), respectively.

$$P_{out}(t) = P_{in}(t) \times \eta_{inv} \tag{27}$$

$$N_{IN} = \frac{P_{G\_max}}{P_{IN\_max}} \tag{28}$$

where, P_{in} refers to the inverter power input and η_{inv} is the inverter efficiency. P_{G_max} represents the maximum power generated by the hybrid system and P_{IN_max} represents the maximum power that can be supplied by the inverter.

2.5. System economics

2.5.1. Net present cost

The net present cost (NPC) is the sum of initial capital cost (C_{ini}), O&M cost ($C_{O\&M}$), and replacement cost (C_{rep}) minus present salvage value ($C_{salvage}$) that remains unused over the lifetime of the asset. Equation (29) is used to compute the component's NPC.

$$NPC_{component} = C_{ini} + C_{rep} + C_{O\&M} - C_{salvage} \tag{29}$$

The initial cost of any component is the multiplication of number of optimal components (N_{comp}) and capital investment cost $/kW of the component, which is shown by the Equation (30).

$$C_{ini} = N_{comp} \times C_{cap,comp} \tag{30}$$

In addition, the component's replacement cost during its lifetime is represented in Equation (31), whereas $N_{rep\text{-}comp}$ is the number of replacements required for a component during its lifetime, $C_{rep,comp}$ is the replacement cost of the component at the expiry of its lifetime, $LF_{project}$ is the project lifetime, f is the inflation rate, i indicates real discount rate (5 %) and $i^{'}$ is the nominal discount rate.

$$C_{rep} = N_{comp} \times C_{rep,comp} \sum_{j=1}^{N_{rep-comp}} \frac{1}{(1+i)^{LF_{comp} \times j}} \tag{31}$$

The total operation and maintenance cost of the component of during its lifetime can be attained as follows:

$$C_{O\&M} = N_{comp} \times C_{o\&m,comp} \sum_{k=1}^{LF_{project}} \frac{1}{(1+i)^k} \tag{32}$$

where $C_{o\&m,comp}$ is the component's operation and maintenance cost.

The salvage value of any component during its overall lifetime can be calculated as follows:

$$C_{salvage} = C_{rep,comp} \times \frac{R_{rem,comp}}{LF_{comp}}\left(\frac{1}{(1+i)^{LF_{project}}}\right) \tag{33}$$

Whereas,

$$R_{rem,comp} = LF_{comp} - \left[LF_{project} - R_{rep,comp}\right] \tag{34}$$

$$R_{rep,comp} = LF_{comp} \times integer\left[\frac{LF_{project}}{LF_{comp}}\right] \tag{35}$$

In the case of diesel generators, the fuel cost can be calculated by the Equation (36).

$$C_{fuel} = P_{fuel} \times F_{fuel} \sum_{k=1}^{LF_{project}} \frac{1}{(1+i)^k} \tag{36}$$

where P_{fuel} means fuel cost ($/L), and F_{fuel} is the annual fuel consumption (L/year).

The overall cost of the RO unit can be determined as follows [93]:

$$C_{RO} = CC_{RO} + MC_{RO} + CC_{WTa} + TC_{MR} + TC_{Chem} \tag{37}$$

where C_{RO}, CC_{RO}, MC_{RO}, TC_{Chem}, and TC_{MR} are the overall RO cost, capital cost, O&M cost, chemical cost, and replacement cost of the membrane, and CC_{WTa} denotes capital cost of the freshwater tank, correspondingly. In addition, all of the costs can be determined as follows:

$$CC_{RO} = C_{ROD} \times Ca_{WD} \times CRF \tag{38}$$

$$MC_{RO} = C_{Mnt-RO} \times D_{WD} \sum_{k=1}^{LF_{project}} \frac{1}{(1+i)^k} \times CRF \tag{39}$$

$$TC_{MR} = C_{MR} \times Ca_{WD} \times N_{Me} \sum_{k=1}^{LF_{project}} \frac{1}{(1+i)^k} \times CRF \tag{40}$$

$$TC_{Chem} = C_{CH} \times D_{WD} \sum_{k=1}^{LF_{project}} \frac{1}{(1+i)^k} \times CRF \tag{41}$$

$$CC_{WTa} = C_{WTa} \times V_{WTa} \times CRF \tag{42}$$

$$CRF(i,n) = \frac{i(1+i)^n}{(1+i)^n - 1} \tag{43}$$

where C_{ROD} indicates the cost of ROD system ($/m^3/day), Ca_{WD} indicates daily volumetric capacity (m^3/day), and CRF is the capital recovery factor, as shown in Equation (43). Moreover, C_{Mnt-RO} is the maintenance cost of the ROD annually, D_{WD} is the daily water demand, C_{MR} is the membrane replacement cost, and N_{Me} is the number of annual membrane replacements. Furthermore, C_{CH} indicates the chemical cost, and C_{WTa} indicates water tank cost.

2.5.2. Cost of energy

Cost of energy is the essential economic indicator to determine the project viability. In the present study, cost of energy is calculated by

Equation (44) [18].

$$COE = \frac{NPC \times CRF(i,n)}{AnnualEnergyServed}$$

(44)

2.6. Socio-environmental impact

2.6.1. Job creation potential

Renewable energy technologies promote economic growth, women empowerment, entrepreneurship, and ultimately benefit the entire economy [94]. It is critical to determine the societal consequences of integrating hybrid renewable energy systems fostering the widespread adoption of renewable energy while mitigating climate change. In this study, employment opportunities created by integrating the hybrid energy system have been investigated. The job creations rely on the type of system components and their capacity to meet a particular demand. The following equation is used to compute the number of jobs created by a system with *n* components.

$$JC = \sum_n f_{JC,n} \times P_n, n \in PV, Batt, and Backup generators$$

(45)

Where *P* is total capacity of the component, and f_{JC} is the job creation potential of that component. The method proposed by Ram et al. [95] has been adopted as it, amongst other aspects, allows for the inclusion of different dimensions of regional trade and labor productivity through the use of employment multipliers which are based on labor productivity across different regions. The data relevant for calculating the employment factors along with the regional multipliers (SAARC region for this study), can be found in Ref. [95].

2.6.2. Life cycle emission (LCE)

The life cycle emission (LCE) in kg CO_2-eq/yr can be calculated using the following formula [96]:

$$LCE = \sum_m \sum_{i=1}^{T} \psi_m E_{m,i}, m \in \{PV, WT, DG, Batt, Methanation, GS, RO, Electrolyzer\} \quad (46)$$

Where, ψ represents the lifetime CO_2 emission equivalent and *E* represents the amount of energy generated or stored by the individual elements over time T (8760 h). The equivalent LCE (kg CO_2-eq/kWh) includes equivalent CO_2 emissions from the energy used to manufacture, transport, and recycle the system components as well as the combustion of fuel in each DG. The equivalent CO_2 emissions for different HES components are reported in Table 4.

2.6.3. Impact on human health and ecosystem

Damage to human health (DHH) is measured in disability adjusted life years (DALYs), which indicate the years of healthy life lost owing to early death or disability caused by prevalent disease or health problems

Table 4
Equivalent LCE for different hardware components.

HES components	LCE (kg CO_2-eq/kWh)	Reference
Solar PV module	0.045	[97]
Wind turbine	0.011	[97]
Diesel engine	0.880	[98]
Electrolyzer and hydrogen tank	0.011	[99]
Lead acid battery	0.028	[100]
Converter	0	[97]
ROD unit	0.149	[101]
Water storage	0.149	[101]

[102]. The raise in the global mean temperature instigated by GHG emission has damaging effect on ecosystem (DES) as well, resulting in loss of local species, the quantity of which integrated over a year is measured in species·yr unit [103]. The computation of DHH and DES requires estimation of the amount (kg) of different GHGs (CO_2, CO, NO_x, SO_x, etc.) emitted by the fossil fuel-run backup generators in their functional lifetime. With the characterization factors (in DALYs/kg and species·yr/kg units) available from ReCiPe2016 method within the SimaPro software database, the following equation can be used for a specific type of non-renewable generator [104].

$$Damage_d = \sum_e \sum_t^{8760} CF_{d,e} \times R_{e,t}, d \in DHH, DES, and e \in CO_2, NOx, SOx, etc.$$

(47)

Here, CF indicates the characterization factor and R indicates emission of a particular GHG over the year. The estimated damages can be further characterized in monetary terms using the conversion factors proposed by Weidema [105]. These conversion factors essentially signify the economic valuation of the willingness of a typical society to preserve 1 DALY or 1 species·yr [105,106]. Weidema estimated that 1 DALY is worth 74,000 €$_{2003}$, while 1 species·yr has an equivalency of 9,500,000 €$_{2003}$. The currency can be converted to equivalent USD values using a multiplier of 1.07 [107].

2.6.4. Renewable fraction

The renewable fraction (RF) signifies the use of renewable energy to meet the load requirement and is stated by Equation (48) [108], whereas E_{nonren} means non-renewable energy usage to meet the load demand and E_s denotes total energy provided.

$$RF = 1 - \frac{E_{nonren}}{E_s}$$

(48)

2.7. System optimization

2.7.1. Objective function

The purpose of this optimization study is to minimize the proposed system's total net present cost. The objective function is written as follows:

$$F = \min(NPC)$$

(49)

2.7.2. Constraints

Decision variables: The number of integrated components is often considered as the decision variable in sizing optimization of a hybrid renewable energy system, which is subject to predetermined upper and lower bounds for computational efficiency as follows:

$$N_{m,min} \leq N_m \leq N_{m,max}, m \in (PV, WT, DG, BES, Inv)$$

(50)

where N_m represents the number of a system component m, and $N_{m,min}$ and $N_{m,max}$ denotes the minimum and maximum number of system components.

Energy balance: The total hourly electrical energy delivered by HES components must match or exceed the hourly electric load demand.

$$E_{PV}(t) + E_{WT}(t) + E_{DG}(t) \pm E_{BES}(t) \geq E_{Elec}(t) + E_{Excess}(t)$$

(51)

E_{PV}, E_{WT}, E_{DG} and E_{BES} are the electricity production from PV, WT, DG and BES at time step *t*, respectively. Additionally, E_{Elec} and E_{Excess} refer to

the electric demand and excess energy at the same period, respectively.

Storage capacity: Each type of energy storage (Battery, Gas Storage, etc.) incorporated into the hybrid system is limited by the following capacity constraint:

$$E_{ES,min} \leq E_{ES}(t) \leq E_{ES,max} \tag{52}$$

where, $E_{ES,min}$ and $E_{ES,max}$ are the minimum and maximum capacity of the energy storage in question.

System reliability: Loss of power supply probability (LPSP) is a commonly recognized reliability index and in the present study, and is determined by Equation 53 [109].

$$LPSP = \frac{\sum_{t=1}^{T} LPS(t)}{\sum_{t=1}^{T} E_L(t)} \tag{53}$$

Here E_L is the total delivered electrical energy (kWh), and LPS denotes loss of power supply over the period T which is calculated by Equation 54.

$$\sum_{t=1}^{T} LPS(t) = \sum_{t=1}^{T} \left(E_L - \left[E_{ren}(t) + E_{Batt}(t-1) - E_{Batt,min} \right] \right.$$
$$\left. \times \eta_{inv} - E_{DG}(t) \right) \tag{54}$$

2.7.3. Energy management strategy

The energy management system of the hybrid energy system to supply community electricity, fresh drinking water through RO process, and cooking gas is shown in Fig. 3. The input data such as solar irradiation, wind velocity, hourly load data are obtained from HOMER software tool. $E_{net}(t)$ is obtained by subtracting community electric load from the renewable energy at every time step t. If $E_{net}(t)$ is more than zero and battery SOC ($E_{batt}(t)$) at any time t is lower than the battery maximum charge capability ($E_{batt,max}(t)$), the surplus energy is used to charge the battery. After full charging of the battery bank the remaining energy, named as wasted energy or excess energy (EE), is utilized to meet the RO load (RL) and gas load (GL) demand. After meeting all the RL and GL, the remaining portion of the EE is then dumped. At any time
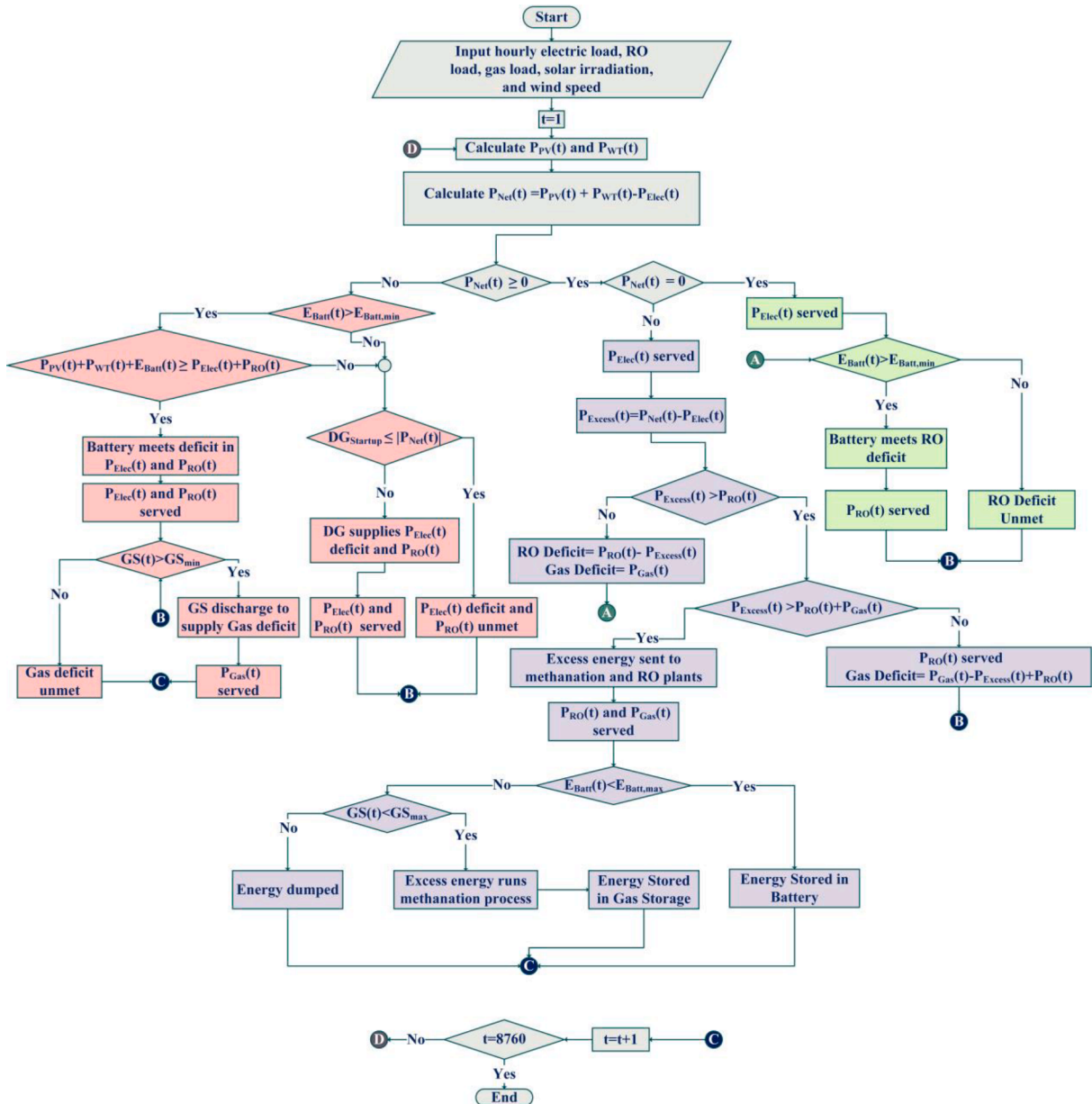

Fig. 3. Energy management strategy for the proposed HES system.

Table 5
Optimization parameters of NSGA-II.

Optimization Parameters	Value
Crossover rate (SBX crossover)	0.9
Mutation rate (Poly mutation)	0.1
Population size	500
Maximum generation	500

step, EE fails to meet the RL and GL, diesel generator and battery is used to fulfill the demand. Furthermore, when $E_{net}(t)$ is equal to zero, therefore no EE is produced. If community electric load is greater than the produced renewable energy as well as the battery SOC ($E_{batt}(t)$) is larger than its minimum level of SOC, the deficit is fulfilled with the battery bank. Additionally, when battery reaches its minimum limit, DG is used to meet the rest of the shortage load such as unmet load of community load, RL, and GL. If the renewable energy and battery band both are incapable to meet the combined load and the shortage load is below the threshold limit of the DG, the shortage demand is named as unmet load which is never met.

2.7.4. Use of non-dominated sorting genetic algorithm II

This study uses non-dominated sorting genetic algorithm-II, commonly known as NSGA-II, for optimizing the proposed system configuration. A well-known and vastly applied evolutionary algorithm in optimization studies, NSGA-II offers an elitist strategy, allowing faster convergence towards the optimal solution. Furthermore, the algorithm is capable of handling larger number of parameters and has been proven more effective in finding the global optima when compared with similar optimization techniques such as PSO [110]. More details of the algorithm can be found in Ref. [111]. In the present study, the optimization is carried out in the MATLAB environment considering the parameters as illustrated in Table 5.

3. Results and discussion

This study reveals the energy management and the optimal sizing of a HES that will satisfy the load demand, freshwater demand and cooking gas demand of Saint Martin, a remote island in Bangladesh. The results of the optimization technique are presented in Table 6.

3.1. Technical performance

As observed from Table 6, minimum size of the PV module (159 kW) is obtained from PV/WT/DG/Batt configuration. The corresponding battery capacity is 437 kWh. The intermittent of solar radiation is

responsible for the high panel capacity. However, when WT is cut off, substantial amount of load needs to be met by the panel thus increasing its size (827 kW). The corresponding battery capacity for PV/Batt configuration is 1887 kWh. The electrolyzer rating is found 139 kW for PV/WT/DG/Batt which is lowest among all the configurations. Maximum electrolyzer rating is found 306 kW which is for PV/Batt configuration. The gas storage for PV/WT/DG/Batt. PV/WT/Batt, PV/Batt and WT/Batt are 360 m^3, 600 m^3, 480 m^3 and 640 m^3, respectively. Therefore, PV/WT/DG/Batt offers the lowest gas storage among all the configurations. The total energy supplied from PV panel in PV/WT/DG/Batt, PV/WT/Batt and PV/Batt are respectively 250,161 kWh, 356,197 kWh, and 1,302,796 kWh. Therefore, minimum energy is supplied by PV panel in PV/WT/DG/Batt configuration. As observed, cutting off DG from PV/WT/DG/Batt configuration results in the larger PV panel sizing and subsequent jump in the excess energy generation (42.39 %). Moreover, further exclusion of WT from the configuration leads to more excess energy production (420.78 %). The increase in excess energy generation is evident as cutting of WT compels the algorithm to implement larger PV panels to produce the required amount of energy. Cutting WT from the configuration increases the gas storage as well as the electrolyzer rating. Therefore, minimum sizing of the component can be achieved by PV/WT/DG/Batt configuration. The hourly resolved operation of the HES configuration for a typical day is illustrated in Fig. 4.

Along the Y-axis, stacked bars in positive direction indicate power produced by the components as well as discharging action of the storage devices in meeting the demands, while those in the negative direction indicates charging action of these devices.

3.2. Economic assessment

Fig. 5 illustrates the convergence of various HES configurations and in all scenarios, they have converged by reaching maximum of 500 generations. It is obvious that the PV/WT/DG/Batt system has the lowest NPC among the different systems studied. Besides, Fig. 6 and Fig. 7 represent the COE and NPC of different configurations, respectively. The COE is found to be minimum for PV/WT/DG/Batt configuration (0.1724 $/kWh) and maximum for the PV/Batt configuration (0.4037 $/kWh). The COE of PV/Batt configuration is even higher than that of WT/Batt configuration (0.3061 $/kWh). Generally, the intermittent nature of solar radiation is responsible for larger PV panel size. Due to cutting of WT and DG from the configuration increases the size of PV panel substantially resulting in the high COE and capital cost. For this reason, PV/Batt configuration has the most COE among all the configurations. The same situation goes for the NPC as observed from Fig. 7. As the cost associated with the PV panel is larger than that of the WT, NPC of PV/Batt is the highest (231,0672 $) compared to other configurations.
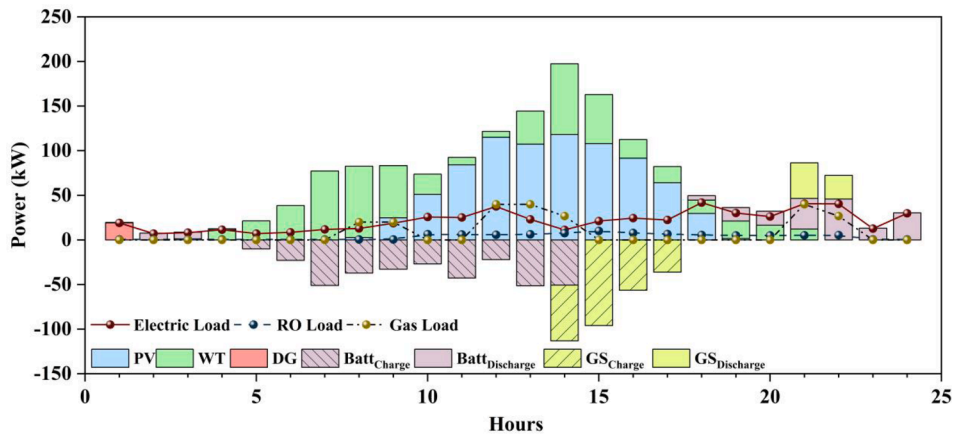
Table 6
Results of the optimal HES for different techniques.

	PV/WT/DG/Batt	PV/WT/Batt	PV/Batt	WT/Batt
COE ($/kWh)	0.1724	0.1879	0.4037	0.3061
TNPC ($)	102,0155	115,4501	231,0672	182,1824
COW ($/m^3)	1.185	1.253	2.088	1.77
COG ($/m^3)	3.978	4.9474	8.45	7.617
PV (kW)	159	226	827	–
WT (kW)	100	100	–	310
DG (kW)	60	–	–	–
RO Capacity (m^3)	20	20	20	20
Battery Capacity (kWh)	437	916	1887	2102
Battery Energy (kWh/yr)	2,511,357	6,415,853	13,740,715	15,968,981
PV energy (kWh/yr)	250,161	356,197	130,279,6	–
WT energy (kWh/yr)	352,056	352,056	–	109,137,4
DG energy (kWh/yr)	328,44	–	–	–
Electrolyzer (kW)	139	194	306	241
Gas storage (m^3)	360	600	480	640
Electrolyzer (kWh/yr)	67,416	73,106	75,165	73,863
Gas Storage (kWh/yr)	30,061	31,286	29,464	33,391
RO Energy (kWh/yr)	31,974	31,974	31,974	31,974

Fig. 4. Hourly resolved operation of the PV/WT/DG/Batt configuration in a typical day.
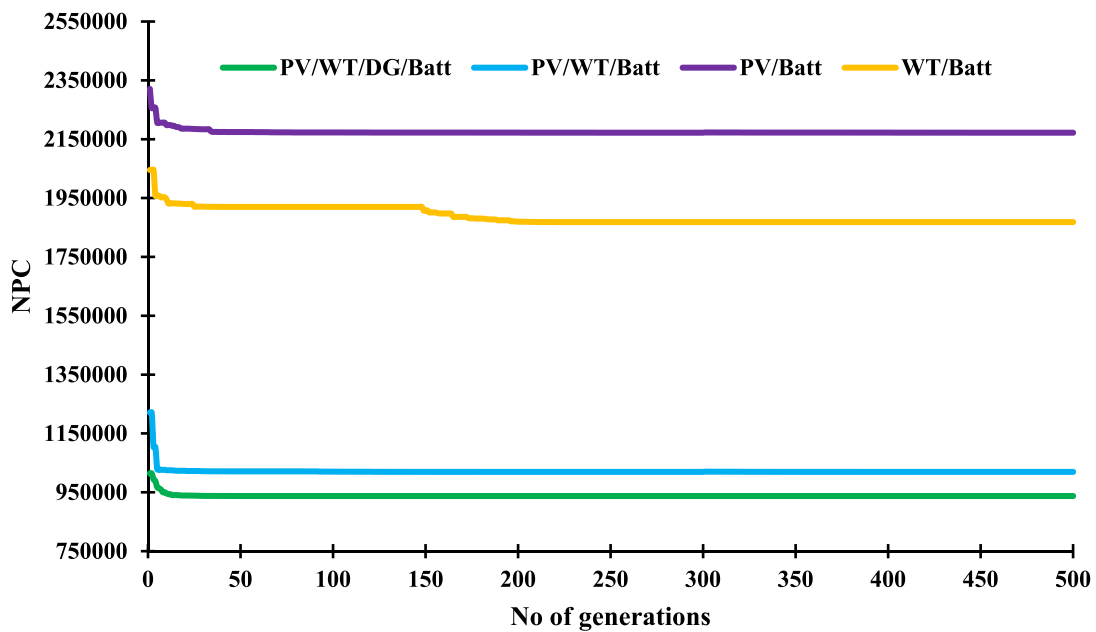

Fig. 5. Convergence of different HES configurations.
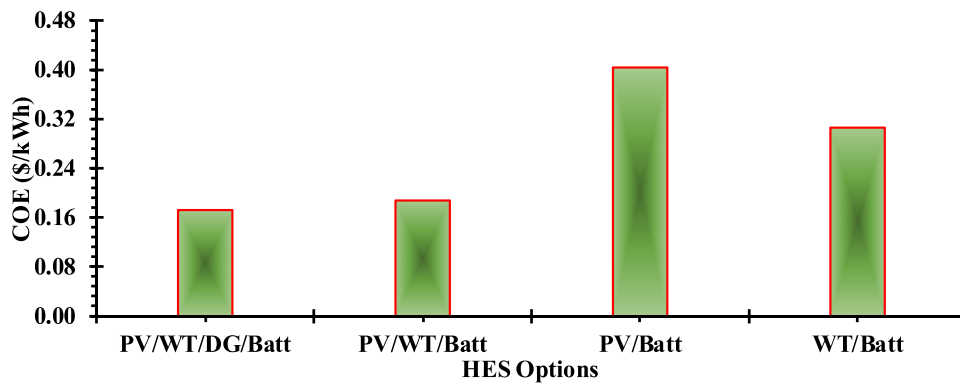

Fig. 6. COE of different HES configurations.

Minimum NPC is associated with PV/WT/DG/Batt configuration (102,0155) as expected due to the minimum sizing of all the components. The COE of PV/WT/DG/Batt is 8.99 %, 134.16 % and 77.55 % lower than those of the PV/WT/Batt, PV/Batt and WT/Batt configurations, respectively. Tehrani et al. [112] reported the COE of 0.24 $/kWh for PV/WT/DG/Batt when meeting the electric load demand only in Kavat, Iran and the HES generated 18.7 % excess energy. However, the PV/WT/Batt and PV/Batt systems generated substantial
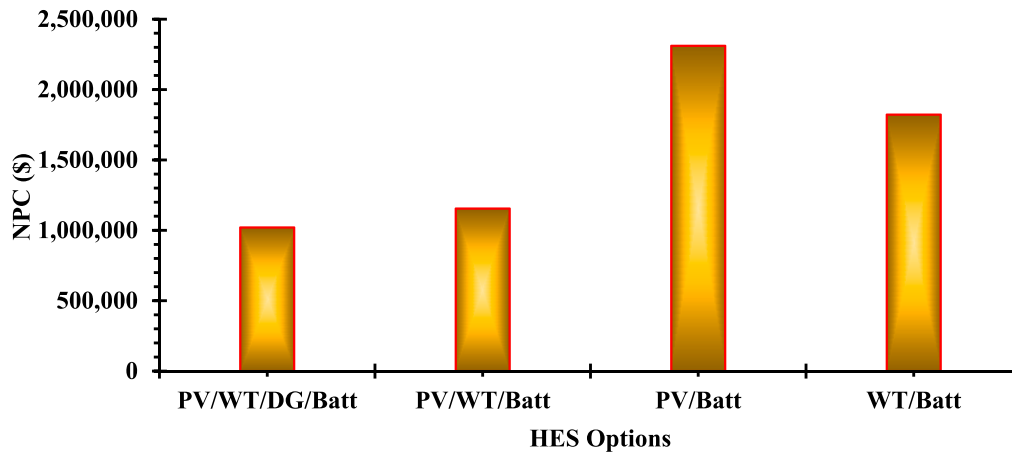
Fig. 7. NPC of different HES configurations.
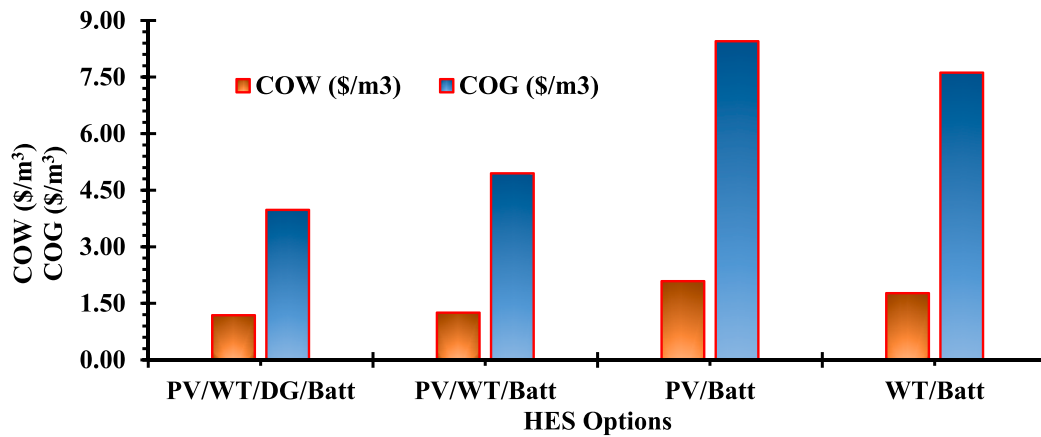
Fig. 8. COW and COG of different HES configurations.

excess energy of 57.6 %, and 67.5 %, respectively. Therefore, the project can be further benefited utilising the excess energy to meet demands like electric vehicle, water desalination or meeting the hydrogen demand.

Fig. 8 represents the cost of water (COW) and cost of gas (COG) of different configurations. Similar to the COE and NPC, the COW (1.185

$/m^3) and COG (3.978 $/m^3) are minimum for PV/WT/DG/Batt configuration due minimum sizing of the components. The higher cost associated with larger PV panel for PV/Batt configuration is responsible for maximum COW (2.088 $/m^3) and COG (8.450 $/m^3) among all the configurations. The COW of PV/WT/DG/Batt is 5.74 %, 76.20 % and 49.37 % lower than those of the PV/WT/Batt, PV/Batt and WT/Batt configurations, respectively. Besides, the COG of PV/WT/DG/Batt is 24.37 %, 112.42 % and 91.48 % lower than those of the PV/WT/Batt, PV/Batt and WT/Batt configurations, respectively. Therefore, PV/WT/DG/Batt is the most economical HES option for the selected area.

3.3. Socio-Environmental impact

This study focused on the job creation potential of the different HES configurations as well as the effect on human health and ecosystem. Life cycle emission (LCE) has been taken into account for evaluating the environmental impact. Later, damage to the human health (DHH) and damaging effect on ecosystem (DES) have been calculated for each of the configurations.

3.3.1. Job creation

In this work, job creation, one of the important social benefit factors, has been calculated for each optimized condition. The potential of a system to create jobs rely on the job creation factor. The higher is the job creation factor, the higher is the potential to create jobs. Fig. 9 represents the JC potentials of different optimized HES configurations. Job creation relies on the capacity of different components to be implemented in the hybrid system. All the four configurations considered in
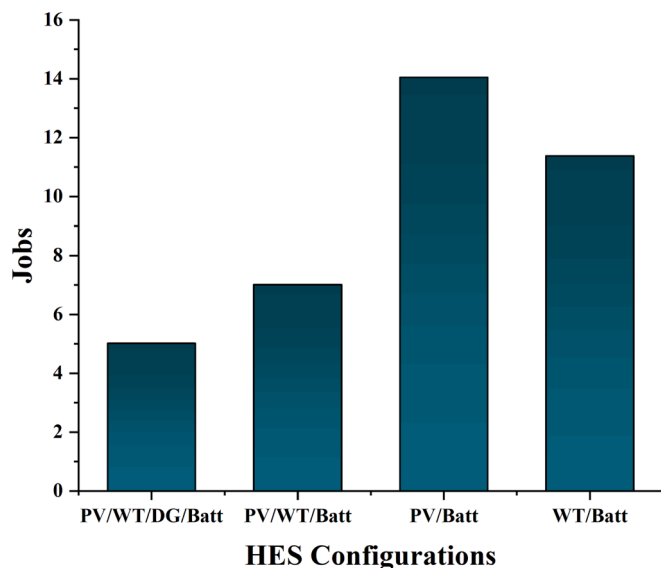

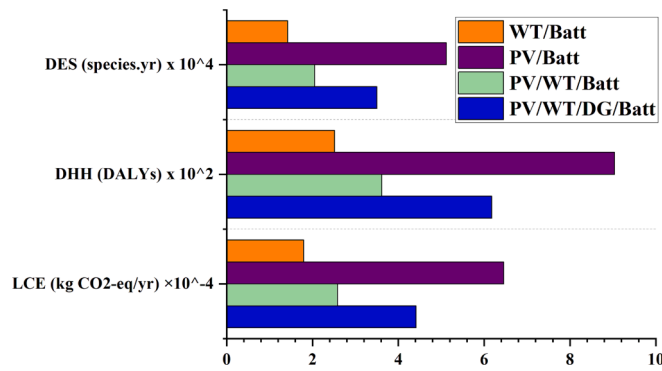**Fig. 9.** Job creation potential of different HES configurations.

Fig. 10. Effect of different HES configurations on environment and human health.

this research will fulfill the load and water demand considered in this study. As PV/Batt offers minimum sizing of the components, it will create the least jobs (5.02) as observed from the figure. However, the excess energy generation is maximum for PV/Batt configuration and the size of the PV panel (827 kW) is also the maximum. Moreover, the job creation factor of PV module is 2.7 jobs/MW than the wind turbine 1.1 jobs/MW [113]. In a PV/WT/Batt option consists of PV module with the capacity of 226 kW, wind turbine capacity of 100 kW, and the battery capacity of 916 kWh, whereas in the PV/Batt system has a PV capacity of 827 kW and the battery capacity of 1887 kWh. Therefore, the PV/Batt option creates the higher jobs opportunities (14.05) than the PV/WT/Batt system. Roy [81] also reported that the PV/Batt offers maximum employment opportunities than the other HES configurations. Implementation of the HES system in the selected region will also bring down several social benefits. For example, the business situation will improve in the island due to the reliable supply of power in both day and night [96]. Moreover, it will also increase the literacy rate of the island by increasing the participation in study due to the continuous supply of electricity.

3.3.2. Environmental impact

The environmental impact of different HES configurations has been analyzed and interpreted in this section. The overall life cycle emission

(LCE), damage to human health (DHH) and damaging effect on ecosystem (DES) of different HES configurations have been summarized in Fig. 10. The emission from PV/Batt is the highest (64540.87 kg CO_2-eq/yr) among all the configurations due to the very large size of the components and larger energy generation. Although, PV/WT/DG/Batt configuration has the greatest number of components, the emission from it is not the highest (44121.25 kg CO_2-eq) due to the minimum size of the components. The emission from WT/Batt configuration is the lowest (17949.03 kg CO_2-eq) as expected due to the elimination of PV panel and diesel generator from the configuration. Moreover, just like LCE, PV/Batt system inflicts the most damage on human health (0.09 DALYs) due to the most contribution in the emission. WT/Batt inflicts least damage on human health (0.03 DALYs) as observed from Fig. 10.

Similarly, PV/Batt system inflicts the most damage on ecosystem (5.12E-04 species.yr) while WT/Batt inflicts the least damage (1.42E-04 species.yr). The approximate worths of the damages by HES configurations are illustrated in Fig. 11. For the selected region, the damage on human health is worth 7154 \$ and the damage on ecosystem is worth 5202 \$ for PV/Batt configuration which are the highest among all the configurations due to the maximum emission of pollutants.

3.4. Best system configuration

This study compares four different HES configurations that will meet the load demand of Saint Martin Island in Bangladesh alongside water and gas demand. Socio-environmental analysis has been performed alongside cost analysis to select the best configuration for the selected area. The PV/WT/DG/Batt configuration has been found the most economic configuration with the lowest COE (0.1724 \$/kWh) which is 9 % lower than PV/WT/Batt configuration which has the second lowest COE. Similarly, the COW and COG of the PV/WT/DG/Batt configuration are the lowest among all the configurations. However, the emission of PV/WT/DG/Batt is 41.49 % higher than that of the PV/WT/Batt for using diesel generator. Although the LCE of WT/Batt configuration is the lowest and is 43.82 % lower than that of PV/WT/Batt system, its COE is 38.61 % higher, which needs to be taken into consideration. Moreover, PV/WT/Batt system inflicts less damage on human health and ecosystem due to lower emission than the PV/WT/DG/Batt system. Therefore, this study concludes PV/WT/DG/Batt to be the best method due to the lowest cost of energy with a slightly higher emission due to the use of
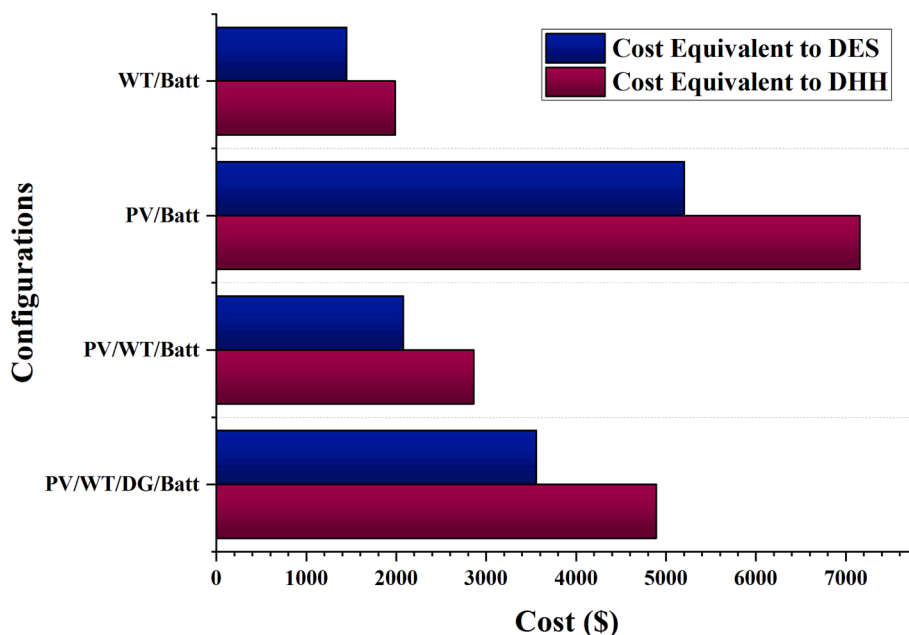

Fig. 11. The monetary valuation of the damage inflicted on ecosystem and human health.
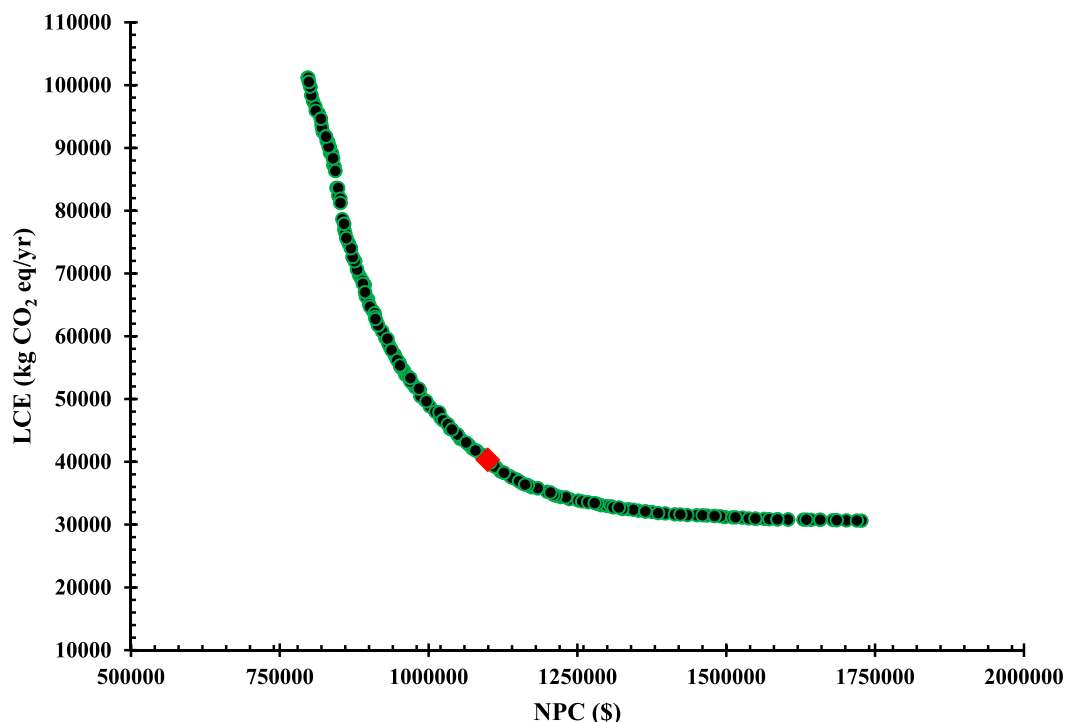
Fig. 12. Pareto front for PV/WT/DG/Batt-based hybrid system. The red point on the Pareto front represents the best trade-off (final solution) using the TOP-SIS method.

Table 7
Comparative analysis of single vs multi-objective optimization techniques.

	NPC ($)	LCE (kg CO₂-eq/yr)	COE ($/kWh)	COW ($/m³)	COG ($/m³)	PV (kW)	WT (kW)	DG (kW)	Batt (kWh)	Electrolyzer (kW)
Single objective (NPC)	1,020,155	44,121	0.1724	1.185	3.978	159	100	60	437	139
Multi-objective (NPC and LCE)	1,110,783	38,734	0.1842	1.236	4.563	170	110	30	784	160

diesel generator for backup. It also offers the lowest COW and COG and offers the minimum size of the components.

The study further extended to examine the impact of HES sizing when multi-objective functions of NPC and LCE for the PV/WT/DG/Batt-based system is considered. The Pareto front for this analysis is reported in Fig. 12, where the final solution (in red color) is achieved using TOPSIS method. The details about TOPSIS method can be retrieved from [114]. The results revealed that the HES has a higher NPC of 1,110,783$ and a lower LCE of 38,734 kg CO₂-eq/yr than the single optimization technique. Additionally, the COE, COW, and COG are 0.1842 $/kWh, 1.236 $/m³, and 4.563 $/m³, respectively as reported in Table 7. It is clearly evident that the cost optimization (single objective function) only has lower energy costs than the multi-objective optimization technique, where cost and emissions are optimized. However, the emissions are fewer in later one than the former technique. Therefore, the HES should be carefully optimized based on the user's preference for cost-effective and sustainable solutions.

3.5. Comparison with literature

The economic evaluation of the four optimized HES suggests that the PV/WT/DG/Batt offers the least cost of energy of 0.1724 $/kWh with a life cycle emission of 44121.25 kg CO₂-eq/yr. The performance of this configuration is further validated by the recently published works. The work performed by Liu et al. [47] used heuristic algorithm to optimize a PV/DG/BES system to supply electricity and water and the best outcome had the COE of 0.2650 $/kWh with 20,503 kg CO₂-eq/yr emission. A case study in India used PV/BG/PHES/BES system to fulfill the

electricity and water demand and the optimized system had 0.4864 $/kWh cost of energy [33]. In another work, authors used HOMER software to optimize a PV/WT/DG/BES system that offered COE of 0.308 $/kWh with CO₂ emission of 3925 kg/yr [72]. The optimum PV/DG/BES proposed by Wu et al. to meet the electricity and freshwater demand in Iran offered 0.3975 $/kWh COE [78]. Ibrahim et al. [80] optimized a PV/WT/DG/BES system using HOMER that had a COE of 0.2252 $/kWh and was responsible for 15,658 kg CO₂-eq/yr emission. Therefore, the proposed system in this study offers one of the best economic outcomes with a satisfactory emission.

4. Conclusions

This study proposed an off-grid PV/WT/Batt/DG system for simultaneously meeting the electricity, freshwater and cooking gas demand for a remote island in Bangladesh. The system has been optimized using NSGA-II to deliver a reliable and cost-effective way for supplying electricity, freshwater and cooking gas. The findings of this study are:

- PV/WT/Batt/DG system generates minimum excess energy and ensures minimum sizing of all the components. Cutting off DG from this system results in the generation of 42.39 % excess energy. The integration of DG into the HES network generates less excess energy while meeting a certain reliability with the given load requirements.
- Economic assessment of different HES showed that PV/WT/Batt/DG configuration is the most economical one with a COE of 0.1724 $/kWh which is 8.99 %, 134.16 % and 77,55 % lower than the COE of PV/WT/Batt, PV/Batt and WT/Batt configurations, respectively.

The COW and COG of the PV/WT/Batt/DG system are also the lowest among all the four configurations and have been found 1.185 $/m^3 and 3.978 $/m^3, respectively. Therefore, PV/WT/DG/Batt is the most economical configuration for the selected area while meeting the electric, freshwater, and cooking gas demands.

- Due to the minimum sizing of the components for the PV/WT/Batt/DG configuration, it offers minimum jobs (5.02) among all the HES studied. The PV/Batt configuration has the highest job (14.05) opportunities due to the maximum sizing of the components.
- The LCE of the PV/WT/Batt/DG configuration is not the highest (44121.25 kg CO_2-eq/yr) due to the few contributions from the diesel generator and less number of battery storage. The PV/Batt system is responsible for the highest LCE (64540.87 kg CO_2-eq/yr) along with the most damage on human health (0.09 DALYs) and the most damage on ecosystem (5.12E-04 species.yr).
- The single objective with cost optimization offers lower cost (NPC: 1,020,155$) than the multi-objective functions (NPC: 1,110,783$) optimization technique, whereas the environmental benefits can be achieved using the multi-objective optimization with LCE being an objective function. Results outlined that around 12 % less LCE generated from the PV/WT/DG/Batt system in multi-objective option than the single objective one at the cost of COE (7 % higher).

The results of this study conclude the PV/WT/Batt/DG configuration to be the best configuration for being the most economical among all the configurations. Moreover, this configuration also offers the minimum cost of water and cost of gas along with the minimum sizing of the components.

CRediT authorship contribution statement

Mim Mashrur Ahmed: Conceptualization, Methodology, Investigation, Data curation, Writing – original draft. **Barun K. Das:** Conceptualization, Methodology, Software, Supervision, Writing – original draft, Writing – review & editing. **Pronob Das:** Conceptualization, Methodology, Software, Writing – review & editing. **Md Sanowar Hossain:** Writing – review & editing. **Md Golam Kibria:** Writing – review & editing.

Declaration of competing interest

The authors declare that they have no known competing financial interests or personal relationships that could have appeared to influence the work reported in this paper.

Data availability

Data will be made available on request.

References

[1] Odou ODT, Bhandari R, Adamou R. Hybrid off-grid renewable power system for sustainable rural electrification in Benin. Renew Energy 2020;145:1266–79.

[2] Shang J, et al. Optimal configuration of hybrid energy systems considering power to hydrogen and electricity-price prediction: A two-stage multi-objective bi-level framework. Energy 2023;263:126023.

[3] Ahmed EE, Demirci A, Tercan SM. Optimal sizing and techno-enviro-economic feasibility assessment of solar tracker-based hybrid energy systems for rural electrification in Sudan. Renew Energy 2023;205:1057–70.

[4] Jia K, et al. Modeling and optimization of a hybrid renewable energy system integrated with gas turbine and energy storage. Energ Conver Manage 2023;279: 116763.

[5] Abdelhady S. Techno-economic study and the optimal hybrid renewable energy system design for a hotel building with net zero energy and net zero carbon emissions. Energ Conver Manage 2023;289:117195.

[6] Yazdani H, Baneshi M, Yaghoubi M. Techno-economic and environmental design of hybrid energy systems using multi-objective optimization and multi-criteria decision making methods. Energ Conver Manage 2023;282:116873.

[7] *Global Energy Review 2021.* 2021 05.06]; Available from: 2021.05.06 https://www.iea.org/reports/global-energy-review-2021.

[8] Ji M, et al. Optimisation of multi-period renewable energy systems with hydrogen and battery energy storage: A P-graph approach. Energ Conver Manage 2023; 281:116826.

[9] Le TS, et al. Optimal sizing of renewable energy storage: A techno-economic analysis of hydrogen, battery and hybrid systems considering degradation and seasonal storage. Appl Energy 2023;336:120817.

[10] Ibrahim O, et al. Development of fuzzy logic-based demand-side energy management system for hybrid energy sources. Energy Convers Manage: X 2023; 18:100354.

[11] Tebibel H. Methodology for multi-objective optimization of wind turbine/battery/electrolyzer system for decentralized clean hydrogen production using an adapted power management strategy for low wind speed conditions. Energ Conver Manage 2021;238:114125.

[12] Suresh V, Muralidhar M, Kiranmayi R. Modelling and optimization of an off-grid hybrid renewable energy system for electrification in a rural areas. Energy Rep 2020;6:594–604.

[13] Samy M, Mosaad MI, Barakat S. Optimal economic study of hybrid PV-wind-fuel cell system integrated to unreliable electric utility using hybrid search optimization technique. Int J Hydrogen Energy 2021;46(20):11217–31.

[14] Xu C, et al. Data-driven configuration optimization of an off-grid wind/PV/hydrogen system based on modified NSGA-II and CRITIC-TOPSIS. Energ Conver Manage 2020;215:112892.

[15] Liu J, et al. Energy planning of renewable applications in high-rise residential buildings integrating battery and hydrogen vehicle storage. Appl Energy 2021; 281:116038.

[16] Elkadeem M, et al. A systematic decision-making approach for planning and assessment of hybrid renewable energy-based microgrid with techno-economic optimization: A case study on an urban community in Egypt. Sustain Cities Soc 2020;54:102013.

[17] Akhtari MR, Baneshi M. Techno-economic assessment and optimization of a hybrid renewable co-supply of electricity, heat and hydrogen system to enhance performance by recovering excess electricity for a large energy consumer. Energ Conver Manage 2019;188:131–41.

[18] Das BK, et al. Techno-economic and environmental assessment of a hybrid renewable energy system using multi-objective genetic algorithm: A case study for remote Island in Bangladesh. Energ Conver Manage 2021;230:113823.

[19] Hassan R, Das BK, Al-Abdeli YM. Investigation of a hybrid renewable-based grid-independent electricity-heat nexus: Impacts of recovery and thermally storing waste heat and electricity. Energ Conver Manage 2022;252:115073.

[20] Das P, et al. Evaluating the prospect of utilizing excess energy and creating employments from a hybrid energy system meeting electricity and freshwater demands using multi-objective evolutionary algorithms. Energy 2022;238: 121860.

[21] Atallah MO, et al. Operation of conventional and unconventional energy sources to drive a reverse osmosis desalination plant in Sinai Peninsula. *Egypt* Renew Energy 2020;145:141–52.

[22] Elkadeem M, et al. Feasibility analysis and optimization of an energy-water-heat nexus supplied by an autonomous hybrid renewable power generation system: An empirical study on airport facilities. Desalination 2021;504:114952.

[23] Sanaye S, Sarrafi A. Cleaner production of combined cooling, heating, power and water for isolated buildings with an innovative hybrid (solar, wind and LPG fuel) system. J Clean Prod 2021;279:123222.

[24] Yusuf A, et al. Multi-objective optimization of concentrated Photovoltaic-Thermoelectric hybrid system via non-dominated sorting genetic algorithm (NSGA II). Energ Conver Manage 2021;236:114065.

[25] Hassan R, Das BK, Al-Abdeli YM. Investigation of a hybrid renewable-based grid-independent electricity-heat nexus: Impacts of recovery and thermally storing waste heat and electricity. Energ Conver Manage 2021:115073.

[26] Alshammari N, Asumadu J. Optimum unit sizing of hybrid renewable energy system utilizing harmony search, Jaya and particle swarm optimization algorithms. Sustain Cities Soc 2020;60:102255.

[27] Sadeghi D, Naghshbandy AH, Bahramara S. Optimal sizing of hybrid renewable energy systems in presence of electric vehicles using multi-objective particle swarm optimization. Energy 2020;209:118471.

[28] Bouakkaz A, et al. Efficient energy scheduling considering cost reduction and energy saving in hybrid energy system with energy storage. J Storage Mater 2021; 33:101887.

[29] Singh S, Chauhan P, Singh N. Capacity optimization of grid connected solar/fuel cell energy system using hybrid ABC-PSO algorithm. Int J Hydrogen Energy 2020.

[30] Jahannoosh M, et al. New hybrid meta-heuristic algorithm for reliable and cost-effective designing of photovoltaic/wind/fuel cell energy system considering load interruption probability. J Clean Prod 2021;278:123406.

[31] Salameh T, et al. Optimal selection and management of hybrid renewable energy System: Neom city as a case study. Energ Conver Manage 2021;244:114434.

[32] Islam M, et al. Techno-economic Optimization of a Zero Emission Energy System for a Coastal Community in Newfoundland, Canada. Energy 2021;119709.

[33] Das M, Singh MAK, Biswas A. Techno-economic optimization of an off-grid hybrid renewable energy system using metaheuristic optimization approaches–case of a radio transmitter station in India. Energ Conver Manage 2019;185:339–52.

[34] Sanajaoba S. Optimal sizing of off-grid hybrid energy system based on minimum cost of energy and reliability criteria using firefly algorithm. Sol Energy 2019; 188:655–66.

[35] Wang Y, et al. Optimal operation of microgrid with multi-energy complementary based on moth flame optimization algorithm. Energy Sources Part A 2020;42(7): 785–806.

[36] Samy M, Barakat S, Ramadan H. A flower pollination optimization algorithm for an off-grid PV-Fuel cell hybrid renewable system. Int J Hydrogen Energy 2019;44 (4):2141–52.

[37] Jamshidi M, Askarzadeh A. Techno-economic analysis and size optimization of an off-grid hybrid photovoltaic, fuel cell and diesel generator system. Sustain Cities Soc 2019;44:310–20.

[38] Secanell M, Wishart J, Dobson P. Computational design and optimization of fuel cells and fuel cell systems: A review. J Power Sources 2011;196(8):3690–704.

[39] Yang H, et al. Optimal sizing method for stand-alone hybrid solar–wind system with LPSP technology by using genetic algorithm. Sol Energy 2008;82(4):354–67.

[40] Mokheimer EM, et al. A new study for hybrid PV/wind off-grid power generation systems with the comparison of results from homer. Int J Green Energy 2015;12 (5):526–42.

[41] Diaf S, et al. A methodology for optimal sizing of autonomous hybrid PV/wind system. Energy Policy 2007;35(11):5708–18.

[42] Borowy BS, Salameh ZM. Methodology for optimally sizing the combination of a battery bank and PV array in a wind/PV hybrid system. Energy Convers, IEEE Trans 1996;11(2):367–75.

[43] Elmorshedy MF, et al. Optimal design and energy management of an isolated fully renewable energy system integrating batteries and supercapacitors. Energ Conver Manage 2021;245:114584.

[44] Razmjoo A, et al. A Technical analysis investigating energy sustainability utilizing reliable renewable energy sources to reduce CO2 emissions in a high potential area. Renew Energy 2021;164:46–57.

[45] Arévalo P, et al. Energy control and size optimization of a hybrid system (photovoltaic-hidrokinetic) using various storage technologies. Sustain Cities Soc 2020;52:101773.

[46] Cai W, et al. Optimal sizing and location based on economic parameters for an off-grid application of a hybrid system with photovoltaic, battery and diesel technology. Energy 2020:117480.

[47] Liu H, Wu B, Maleki A. Effects of dispatch strategies on optimum sizing of solar-diesel-battery energy storage-RO desalination hybrid scheme by efficient heuristic algorithm. J Storage Mater 2022;54:104862.

[48] Wu Y, Zhong L. An integrated energy analysis framework for evaluating the application of hydrogen-based energy storage systems in achieving net zero energy buildings and cities in Canada. Energ Conver Manage 2023;286:117066.

[49] Kahwash F, Barakat B, Maheri A. Coupled thermo-electrical dispatch strategy with AI forecasting for optimal sizing of grid-connected hybrid renewable energy systems. Energ Conver Manage 2023;293:117460.

[50] Rad MAV, et al. Excess electricity problem in off-grid hybrid renewable energy systems: A comprehensive review from challenges to prevalent solutions. Renew Energy 2023.

[51] Shafiullah G, et al. Prospects of hybrid renewable energy-based power system: A case study, post analysis of Chipendeke Micro-Hydro. *Zimbabwe* IEEE Access 2021;9:73433–52.

[52] Ali M, et al. Techno-economic assessment and sustainability impact of hybrid energy systems in Gilgit-Baltistan. *Pakistan* Energy Reports 2021;7:2546–62.

[53] Ampah JD, et al. Performance analysis and socio-enviro-economic feasibility study of a new hybrid energy system-based decarbonization approach for coal mine sites. Sci Total Environ 2023;854:158820.

[54] Wulf C, Linßen J, Zapp P. Review of power-to-gas projects in Europe. Energy Proc 2018;155:367–78.

[55] Koj JC, Wulf C, Zapp P. Environmental impacts of power-to-X systems-A review of technological and methodological choices in Life Cycle Assessments. Renew Sustain Energy Rev 2019;112:865–79.

[56] Gong J, et al. Power-to-X: lighting the path to a net-zero-emission future. ACS Publications; 2021. p. 7179–81.

[57] Sorrenti I, et al. The role of power-to-X in hybrid renewable energy systems: A comprehensive review. Renew Sustain Energy Rev 2022:112380.

[58] Incer-Valverde J, et al. Hydrogen-driven Power-to-X: State of the art and multicriteria evaluation of a study case. Energ Conver Manage 2022;266:115814.

[59] Turk A, et al. Optimal operation of integrated electrical, district heating and natural gas system in wind dominated power system. Int J Smart Grid Clean Energy 2020;9(2):237–46.

[60] Onodera H, Delage R, Nakata T. Systematic effects of flexible power-to-X operation in a renewable energy system-A case study from Japan. Energy Convers Manage: X 2023;20:100416.

[61] Li X, et al. Sustainable energy ecosystem based on Power to X technology. in Int. Conf. Appl. Energy. 2019.

[62] Xu X, et al. Enhanced design of an offgrid PV-battery-methanation hybrid energy system for power/gas supply. Renew Energy 2021;167:440–56.

[63] Gillessen B, et al. Hybridization strategies of power-to-gas systems and battery storage using renewable energy. Int J Hydrogen Energy 2017;42(19):13554–67.

[64] Dezhdar A, et al. Transient optimization of a new solar-wind multi-generation system for hydrogen production, desalination, clean electricity, heating, cooling, and energy storage using TRNSYS. Renew Energy 2023;208:512–37.

[65] Mustafa J, et al. Effect of economic and environmental parameters on multi-generation of electricity, water, heat, and hydrogen in Saudi Arabia: A case study. Int J Hydrogen Energy 2023.

[66] Al-Orabi AM, Osman MG, Sedhom BE. Evaluation of green hydrogen production using solar, wind, and hybrid technologies under various technical and financial scenarios for multi-sites in Egypt. Int J Hydrogen Energy 2023.

[67] Bukhari MH, et al. Techno-economic feasibility analysis of hydrogen production by PtG concept and feeding it into a combined cycle power plant leading to sector coupling in future. Energ Conver Manage 2023;282:116814.

[68] He H, et al. Potential and economic viability of green hydrogen production from seawater electrolysis using renewable energy in remote Japanese islands. Renew Energy 2023;202:1436–47.

[69] Nasrabadi AM, Korpeh M. Techno-economic analysis and optimization of a proposed solar-wind-driven multigeneration system; case study of Iran. Int J Hydrogen Energy 2023;48(36):13343–61.

[70] Javed MS, et al. Economic analysis and optimization of a renewable energy based power supply system with different energy storages for a remote island. Renew Energy 2021;164:1376–94.

[71] Mayer MJ, Szilágyi A, Gróf G. Environmental and economic multi-objective optimization of a household level hybrid renewable energy system by genetic algorithm. Appl Energy 2020;269:115058.

[72] Gökçek M. Integration of hybrid power (wind-photovoltaic-diesel-battery) and seawater reverse osmosis systems for small-scale desalination applications. Desalination 2018;435:210–20.

[73] Padrón I, et al. Assessment of Hybrid Renewable Energy Systems to supplied energy to Autonomous Desalination Systems in two islands of the Canary Archipelago. Renew Sustain Energy Rev 2019;101:221–30.

[74] Li Q, et al. Sustainable and reliable design of reverse osmosis desalination with hybrid renewable energy systems through supply chain forecasting using recurrent neural networks. Energy 2019;178:277–92.

[75] Alirahmi SM, Rostami M, Farajollahi AH. Multi-criteria design optimization and thermodynamic analysis of a novel multi-generation energy system for hydrogen, cooling, heating, power, and freshwater. Int J Hydrogen Energy 2020;45(30): 15047–62.

[76] Abdelshafy AM, Hassan H, Jurasz J. Optimal design of a grid-connected desalination plant powered by renewable energy resources using a hybrid PSO–GWO approach. Energ Conver Manage 2018;173:331–47.

[77] Rosales-Asensio E, et al. Stress mitigation of conventional water resources in water-scarce areas through the use of renewable energy powered desalination plants: An application to the Canary Islands. Energy Rep 2020;6:124–35.

[78] Wu B, et al. Optimal design of stand-alone reverse osmosis desalination driven by a photovoltaic and diesel generator hybrid system. Sol Energy 2018;163:91–103.

[79] Mehrjerdi H. Modeling and optimization of an island water-energy nexus powered by a hybrid solar-wind renewable system. Energy 2020;197:117217.

[80] Ibrahim MM, et al. Performance analysis of a stand-alone hybrid energy system for desalination unit in Egypt. Energ Conver Manage 2020;215:112941.

[81] Roy D. Modelling an off-grid hybrid renewable energy system to deliver electricity to a remote Indian island. Energ Conver Manage 2023;281:116839.

[82] Hossain M, Mekhilef S, Olatomiwa L. Performance evaluation of a stand-alone PV-wind-diesel-battery hybrid system feasible for a large resort center in South China Sea. *Malaysia* Sustain cities Soc 2017;28:358–66.

[83] Mainali B, Ahmed H, Silveira S. Integrated approach for provision of clean energy and water in rural Bangladesh. Groundw Sustain Dev 2018;7:239–49.

[84] Islam M, et al. Techno-economic optimization of a zero emission energy system for a coastal community in Newfoundland. *Canada* Energy 2021;220:119709.

[85] Xu X, et al. Optimal operational strategy for an offgrid hybrid hydrogen/electricity refueling station powered by solar photovoltaics. J Power Sources 2020;451:227810.

[86] Li C-H, et al. Dynamic modeling and sizing optimization of stand-alone photovoltaic power systems using hybrid energy storage technology. Renew Energy 2009;34(3):815–26.

[87] Zeng Q, et al. Steady-state analysis of the integrated natural gas and electric power system with bi-directional energy conversion. Appl Energy 2016;184: 1483–92.

[88] Veluswamy HP, et al. A review of solidified natural gas (SNG) technology for gas storage via clathrate hydrates. Appl Energy 2018;216:262–85.

[89] Liu W, et al. Comprehensive feasibility study of two-well-horizontal caverns for natural gas storage in thinly-bedded salt rocks in China. Energy 2018;143: 1006–19.

[90] Johnson GL. Wind energy systems. Citeseer; 1985.

[91] *Lead acid battery* [cited 23 20.08]; Available from: 20. 08.2023 https://www. rollsbattery.com/wp-content/uploads/2019/11/Rolls-Battery-Renewable-Energy.pdf.

[92] Gharibi M, Askarzadeh A. Size and power exchange optimization of a grid-connected diesel generator-photovoltaic-fuel cell hybrid energy system considering reliability, cost and renewability. Int J Hydrogen Energy 2019;44 (47):25428–41.

[93] Maleki A. Design and optimization of autonomous solar-wind-reverse osmosis desalination systems coupling battery and hydrogen energy storage by an improved bee algorithm. Desalination 2018;435:221–34.

[94] Gatto A, Drago C. When renewable energy, empowerment, and entrepreneurship connect: Measuring energy policy effectiveness in 230 countries. Energy Res Soc Sci 2021;78:101977.

[95] Ram M, et al. Job creation during a climate compliant global energy transition across the power, heat, transport, and desalination sectors by 2050. Energy 2022; 238:121690.

[96] Roy D, Hassan R, Das BK. A hybrid renewable-based solution to electricity and freshwater problems in the off-grid Sundarbans region of India: Optimum sizing and socio-enviro-economic evaluation. J Clean Prod 2022;372:133761.

[97] Katsigiannis YA, Georgilakis P, Karapidakis E. Multiobjective genetic algorithm solution to the optimum economic and environmental performance problem of small autonomous hybrid power systems with renewables. IET Renew Power Gener 2010;4(5):404–19.

[98] Dones R, Heck T, Hirschberg S. Greenhouse gas emissions from energy systems: comparison and overview. 2004.

[99] Khan FI, Hawboldt K, Iqbal M. Life cycle analysis of wind–fuel cell integrated system. Renew Energy 2005;30(2):157–77.

[100] Rydh CJ. Environmental assessment of vanadium redox and lead-acid batteries for stationary energy storage. J Power Sources 1999;80(1–2):21–9.

[101] Clarke DP, Al-Abdeli YM, Kothapalli G. Multi-objective optimisation of renewable hybrid energy systems with desalination. Energy 2015;88:457–68.

[102] WHO methods and data sources for global burden of disease estimates 2000-2019. December 2020, Department of Data and Analytics, World Health Organization.

[103] Huijbregts MAJ. ReCiPe 2016, A harmonized life cycle impact assessment method at midpoint and endpoint level. 2016, National Institute for Public Health and the Environment.

[104] Huijbregts MA, et al. ReCiPe2016: a harmonised life cycle impact assessment method at midpoint and endpoint level. Int J Life Cycle Assess 2017;22:138–47.

[105] Weidema BP. Comparing three life cycle impact assessment methods from an endpoint perspective. J Ind Ecol 2015;19(1):20–6.

[106] Cobo S, et al. Human and planetary health implications of negative emissions technologies. Nat Commun 2022;13(1):2535.

[107] Euro foreign exchange reference rates. [cited 2023 May]; Available from: https://www.ecb.europa.eu/stats/policy_and_exchange_rates/euro_reference_exchange_rates/html/eurofxref-graph-usd.en.html.

[108] Das BK, Tushar MSH, Hassan R. Techno-economic optimisation of stand-alone hybrid renewable energy systems for concurrently meeting electric and heating demand. Sustain Cities Soc 2021;68:102763.

[109] Barakat S, Ibrahim H, Elbaset AA. Multi-objective optimization of grid-connected PV-wind hybrid system considering reliability, cost, and environmental aspects. Sustain Cities Soc 2020;60:102178.

[110] Erdinc O, Uzunoglu M. Optimum design of hybrid renewable energy systems: Overview of different approaches. Renew Sustain Energy Rev 2012;16(3):1412–25.

[111] Deb K, et al. A fast and elitist multiobjective genetic algorithm: NSGA-II. IEEE Trans Evol Comput 2002;6(2):182–97.

[112] Tehrani MM, et al. Techno-economic investigation of a hybrid biomass renewable energy system to achieve the goals of SDG-17 in deprived areas of Iran. Energ Conver Manage 2023;291:117319.

[113] Sawle Y, Gupta S, Bohre AK. Socio-techno-economic design of hybrid renewable energy system using optimization techniques. Renew Energy 2018;119:459–72.

[114] Goh QH, et al. Modelling and multi-objective optimisation of sustainable solar-biomass-based hydrogen and electricity co-supply hub using metaheuristic-TOPSIS approach. Energ Conver Manage 2023;293:117484.